Fe-S clusters masquerading as zinc finger proteins

*Jordan D. Pritts, Sarah L. J. Michel**

[a]Department of Pharmaceutical Sciences, School of Pharmacy, University of Maryland,

Baltimore, Maryland 21201-1180, United States

*To whom correspondence should be addressed. Phone: (410) 706-7038. Fax: (410) 706-

5017. Email: smichel@rx.umaryland.edu

Abstract

Metal ions are commonly found as protein co-factors in biology, and it is estimated that over a quarter of all proteins require a metal cofactor. The distribution and utilization of metals in biology has changed over time. As the earth evolved, the atmosphere became increasingly oxygen rich which affected the bioavailability of certain metals such as iron, which in the oxidized ferric form is significantly less soluble than its reduced ferrous counterpart. Additionally, proteins that utilize metal cofactors for structural purposes grew in abundance, necessitating the use of metal co-factors that are not redox active, such as zinc. One common class of Zn co-factored proteins are zinc finger proteins (ZFs). ZFs bind zinc utilizing cysteine and histidine ligands to promote structure and function. Bioinformatics has annotated 5% of the human genome as ZFs; however, many of these proteins have not been studied empirically. In recent years, examples of annotated ZFs that instead harbor Fe-S clusters have been reported. In this review we highlight four examples of mis-annotated ZFs: mitoNEET, CPSF30, nsp12, and Fep1 and describe methods that can be utilized to differentiate the metal-cofactor.

Key words

Zinc finger, iron-sulfur cluster, metalloprotein, bioinformatics, spectroscopy, metal cofactors

1. Introduction

Metal ions play an important role in biology. One major role for metals is as a protein cofactor, and at least 25% of all proteins are predicted to contain metal co-factors [1-6]. In recent years, new roles for metals in regulation and homeostasis have been identified. Here, metal binding to cognate proteins can be transient, and as a result these proteins are not always annotated as metalloproteins [3, 7-12]. As such, we may be under-estimating the number of 'metalloproteins' in biology.

The distribution and utilization of metals in biology has changed over time. For metalloproteins, as the earth evolved from an anaerobic to an aerobic environment, the introduction of oxygen altered the availability of metals to serve as protein cofactors [4, 13-16]. Ferrous iron (Fe^{2+}), a common co-factor, was now susceptible to oxidation to ferric iron (Fe^{3+}) and to higher order oxidized species (e.g., iron oxy-hydroxides) in the newly O_2-rich aerobic environment. These oxidized forms of iron are less soluble in biological solvents (i.e., buffer, water) making iron less bioavailable [13, 15, 17-20]. Concomitantly, zinc, which is redox inert and therefore not oxygen sensitive, became more prevalent as a co-factor in the aerobic environment [18-20]. A whole class of structural zinc proteins, called zinc finger proteins (ZFs), emerged during this transition [21-23]. One prediction is that these new ZF proteins evolved from iron-co-factored proteins to obviate the reactivity problem of O_2.

The discovery of ZF proteins illustrates how eukaryotic metalloproteins may have evolved by adapting prokaryotic metalloprotein sites. One of the earliest ZFs to be identified in the mid 1980s- was

transcription factor IIIA (TFIIIA) from *Xenopus* oocytes [24-28]. TFIIIA contains nine repeated domains each of which has two conserved cysteine and histidine residues. The domains have an overall consensus sequence of (Tyr, Phe)-X-**Cys**-X_{2-4}-**Cys**-X_3-Phe-X_5-Leu-X_2-**His-**X_{3-4}-**His**-X_{1-6} [29]. TFIIIA was found to be functional only when zinc is present, suggesting that it was a zinc co-factored protein [26]. Zinc is a borderline metal (acid), defined by the hard-soft acid-base theory, and can bind to both hard and soft bases, including cysteinate thiolate (soft) ligands and histidine imidazole (hard) ligands [30-33]. Thus, it was predicted that zinc would bind to the conserved Cys and His ligands within TFIIIA [26, 28, 29]. How zinc binding to these ligands would affect protein structure was not clear. In the mid-1980s, the number of structurally characterized proteins was still fairly low; however, the motif found in TFIIIA did have some counterparts in structurally characterized prokaryotic proteins. As such, the structure of TFIIIA was presciently predicted by Jeremy Berg, who had recently completed his PhD under the tutelage of Richard Holm (**Figure 1**).[*] Berg recognized that the X_2-Cys-X_3-Cys-X_4 half of the conserved CCHH domain present in TFIIIA, was homologous to a sequence found in two structurally characterized proteins: rubredoxin, an iron-cofactored prokaryotic protein, and aspartate transcarbamoylase, a zinc-co-factored prokaryotic protein [34]. In these structures an anti-parallel beta sheet was formed upon metal coordination to the two conserved cysteines. Similarly, Berg recognized that the X_4-His-X_3-His-X_5 half of the CCHH domain of TFIIIA was homologous to sequences found in thermolysin, a prokaryotic zinc-cofactored protein, hemerythrin, an

[*] PhD Richard Holm 1980-1984

iron co-factored protein found in marine invertebrates and hemocyanin, a copper co-factored protein, also found in marine invertebrates. Structures of these proteins revealed an alpha helical fold mediated by the two His ligands and their cognate metal [34]. This was also supported by independent structural prediction models [35]. Based upon these observations, Berg predicted that the TFIIIA ZF would adopt an anti-parallel beta-sheet followed by an alpha helix fold via the CC and HH domains upon zinc binding [27, 28, 34]. This prediction was confirmed by the X-ray structure of ZIF-268 (a homologous ZF protein) and subsequent structures of other CCHH ZFs revealing that this a common fold for CCHH type ZFs [36-38].

At the same time that ZF protein structures were being predicted, efforts to predict structures of other metalloproteins, including zinc metalloenzymes, were underway. It was recognized that while ZFs require four ligands to bind Zn in a tetrahedral geometry, zinc metalloenzymes utilize 3 ligands such that a fourth 'open' site for substrate binding is available. This site is typically occupied by H_2O. Once a handful of zinc metalloenzymes were structurally characterized, it was possible to predict that newly sequenced proteins were zinc metalloenzymes. From the structures coupled with sequence alignments, it was recognized that zinc metalloenzymes utilize a combination of His, Glu, Asp and Cys as ligands and specific spacing between the ligands were identified. These properties were predicted to translate to specific secondary structural features (e.g., alpha helix, beta strand) and specific domain folds. As with all predictions, experimental verification was needed, and subsequent studies focused on this. As this 'focused review' is on ZF proteins with Fe-S sites, we refer the reader to this

excellent *Perspectives* article in Biochemistry along with its large number of citations, for more insight regarding how zinc metalloenzyme structures can be predicted [39].

Since their initial discovery, ZFs have been identified in simple (e.g., yeast) and complex (e.g., human) eukaryotes, where they have been found to be involved in a myriad of biological processes, ranging from transcription to translation to protein regulation [40-43]. These roles are accomplished via a macromolecular binding interaction. The ZF binds to another macromolecule (e.g., DNA) to promote or repress a function (e.g., transcription). ZFs are present in higher numbers the farther you move up the evolutionary tree, which may reflect the increased complexity of these biological systems and increased need for regulation [44]. As more proteins have been identified, new types of ZFs have been discovered. These new ZFs contain variations of cysteine and histidine residues within their domains [40, 41, 45, 46]. The common feature of all ZF proteins is the presence of domains that include four cysteine (Cys) and/or histidine (His) ligands. The Cys/His ligands coordinate zinc in a tetrahedral geometry which results in a folded domain. Today, ZFs are classed based upon their amino acid sequence, cysteine/histidine ratio, spacing of cysteine/histidine residues, fold, and/or binding partners. At least 30 classes have been identified to date [41, 45-50]. The original type of ZF identified by Berg (e.g TFIIIA), is now called a “classical” ZF and the remaining are “nonclassical” [41, 50].

After the human genome was sequenced in the early 2000s, bioinformatics analysis estimated that 5% of the human genome encodes for ZF proteins and that 10% of all human proteins utilize zinc as either a

structural or catalytic co-factor [21, 44, 51-53]. In most cases, these predictions were based upon the protein's amino acid sequence, the presence of specific sequence domains already attributed to ZFs, and crystal and NMR structures, when available [21, 44, 51, 52]. In **table 1**, we provide a count of the annotated ZF proteins reported in studies by Andreni, Decaria, and Passerini, along with a tally of the annotated ZF proteins for which empirical data are available. We also report the number of proteins that are annotated as ZFs when the online databases uniport and geneontology are used to query for ZFs, in order to illustrate the variability in numbers of annotated ZFs.

Although some of these proteins have subsequently been studied empirically and validated as *bona fide* ZFs, many remain putative ZFs. For example, in humans, it is estimated that between 903-3472 human proteins are zinc binding proteins (estimates differ due to different bioinformatics approaches) [21, 44, 51, 52]. Less than 300 of these predicted ZFs have been characterized experimentally, therefore we only have a partial picture of the zinc-finger-ome (**Table 1)**. Notably, not all of the proteins annotated as ZFs have been found to be *bona fide* ZFs when studied empirically. In some instances, annotated 'ZFs' have been found to be Fe-S co-factored proteins[54-57]. Unlike ZFs, proteins that contain Fe-S cluster co-factors do not have a well-defined sequence motif, but many contain a peptide motif, LYR, that interacts directly with the cochaperone involved in Fe-S cluster delivery [58-61]. Like ZFs, proteins with Fe-S cofactors also favor cysteine and histidine ligands, perhaps explaining why some Fe-S co-factored proteins are annotated as ZFs (**Figure 2**) [62, 63]. This is not the first time that the limitations of the prediction of metal co-factors from amino sequence have

been brought to light. For example, as part of the NIH funded protein structure initiative, Prestergard and Adams structurally characterized PF0610, a protein with a helix-turn-helix motif and predicted zinc ribbon domain, that was found to bind both zinc and iron in vitro, with the latter being the proposed in vivo cofactor. Similarly, Eklund and co-workers noted that the zinc binding domain of horse liver alcohol dehydrogenase resembled ferredoxins in 1976 [64, 65]. Together, these findings underscore the importance of empirically validating annotated ZFs.

This review focusses on four examples of proteins that were annotated as ZF proteins but were discovered to have Fe-S cofactors when studied empirically. These proteins are mitoNEET, CPSF30, nsp12, and Fep1. MitoNEET and CPSF30 are eukaryotic proteins, while nsp12 is a viral protein that utilizes the mammalian Fe-S cluster machinery during infection. Fep1 is a fungal protein that belongs to the GATA family of transcription factors, and has homologs in many organisms including slime mold, plants, nematodes, insects, echinoderms, and vertebrates [66]. We describe the work that led to the discoveries that these proteins are Fe-S co-factored proteins, as 'case studies,' after which we provide an overview of experimental methods that were important for the delineation of these proteins' functions.

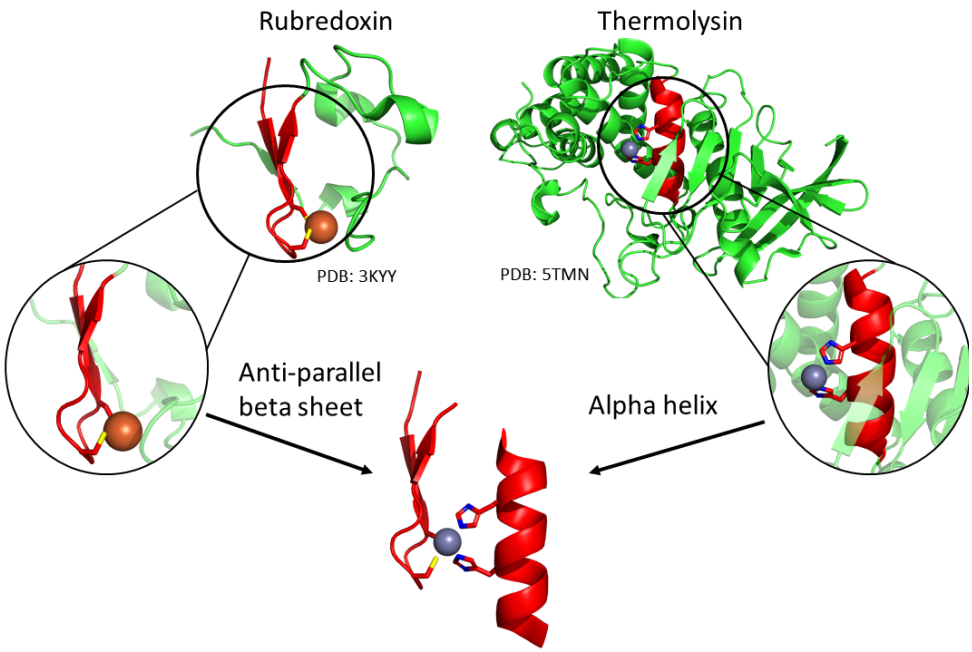

Figure 1. The X-ray structure of rubredoxin (PDB: 3KYY) and thermolysin (PDB: 5TMN) with a focus on the metal centers. The anti-parallel beta sheet from rubredoxin and the alpha helix from thermolysin are shown in red coming together to form the structure of the classical CCHH type ZF, TFIIIA, predicted by Berg. Both proteins were modeled in pymol as cartoons with the cysteines from rubredoxin and the histidines from thermolysin shown as sticks.

Ligand Set	Zn cofactored	Fe-S cofactored
CCCC	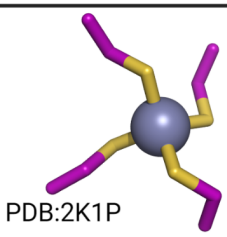 PDB:2K1P	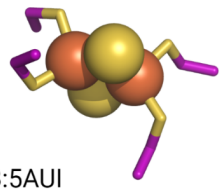 PDB:5AUI
CCCH	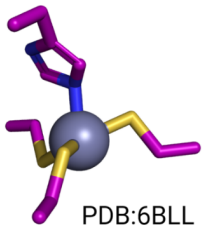 PDB:6BLL	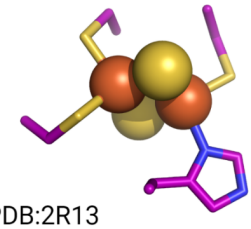 PDB:2R13
CCHH	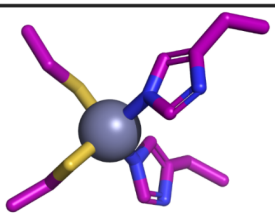 PDB:1A1L	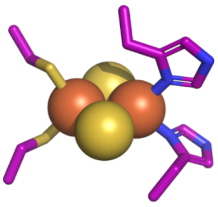 PDB:2NVF

Figure 2. The metal centers of Zn vs Fe-S cluster co-factored proteins with CCCC, CCCH, and CCHH ligand sets. Protein structures of ZRANB2 (PDB:2K1P), ferredoxin (5AUI), CPSF30 (6BLL), mitoNEET (2R13), ZIF268 (1A1L), and Rieske (2NVF) were obtained from the PDB. Pymol was utilized to generate snapshots of each metal center.

Table 1. Summary of papers and databases designed to annotate human zinc binding proteins.

Source	Paper or web database	# of human zinc binding proteins annotated	# of human zinc binding proteins annotated with empirical evidence
Andreini et al, 2006 [51]	Both	3207	N.D.
Andreini et al, 2006 [21]	Paper	3472	N.D.
This work, 2021	Uniprot.org (Swiss-Prot)	2412[1]	202[2]
This work, 2021	Uniprot.org (TrEMBL)	174[3]	N.D.
This work, 2021	Geneontology.org	902[4]	218[5]
Decaria et al, 2010 [44]	Paper	1830 ZFs	N.D.
ZincBind [67]	Database used to query PDB	N.D.	267

Passerini et al, 2007 [52]	Both	2833	N.D.

[1]Database search of Uniprot.com Swiss-Prot with keyword: “Zinc [KW-0862]” AND reviewed:yes AND organism: “Homo sapiens (Human) [9606]” settings. As of December 2021.

[2]Database search of Uniprot.com Swiss-Prot with keyword: “Zinc [KW-0862]” annotation type:metal evidence: “Inferred from experiment [ECO:0000269]”) AND reviewed:yes AND organism: “Homo sapiens (Human) [9606]”. As of December 2021.

[3]Database search of Uniprot.com TrEMBL keyword: “Zinc [KW-0862]" annotation:(type:metal) AND reviewed:no AND organism: “Homo sapiens (Human) [9606]” As of December 2021.

[4]Database search of Geneontology.org utilizing “zinc ion binding” as the search term and “Homo Sapiens” as an “Organism” filter . As of December 2021.

[5] Database search of Geneontology.org utilizing “zinc ion binding” as the search term and “Homo Sapiens” as an “Organism” filter and “Experimental evidence” as an “Evidence” filter. As of December 2021.

2. Case study #1: MitoNEET

MitoNEET is a 108 amino acid protein that was first discovered in 2004 as a target for pioglitazone. Pioglitazone is a member of the thiazolidinediones (TZD) family of drugs which are used to treat type 2 diabetes by increasing sensitivity to insulin [68]. MitoNEET was named based upon its site of cellular localization - the mitochondria – and a conserved Asn-Glu-Glu-Thr or NEET sequence. MitoNEET was annotated as a ZF because it contains a singular 'Cys$_3$His' or CCCH sequence which is a type of "non-classical" ZF domain (**C**-X-**C**-X$_2$-(S/T)-X$_3$-P-X-**C**-D-G-(S/A/T)-**H**). Two homologs, named Miner1 and Miner2 (i.e., MitoNEET-related proteins 1 and 2, Miner2 is now also called MiNT) were also found to contain this putative ZF domain [69, 70]. When recombinant mitoNEET was isolated after expression in *E. coli*, the protein was observed to be a brownish red color which suggested the presence of iron. The metal content measurement of the isolated mitoNEET protein confirmed this prediction: mitoNEET was found to be loaded with 1.6 equivalents of Fe per protein and no Zn [69]. Similarly, when Miner 1 and 2 were recombinantly expressed and purified, analogous Fe and Zn stoichiometry was reported [57]. These findings were unexpected, because the CCCH site present in all three proteins was annotated as a ZF site. Efforts to favor zinc loading by adding excess Zn (5 μM) were unsuccessful: mitoNEET was still isolated with only iron bound [69]. Together, these data provided evidence that mitoNEET is an iron co-factored protein and not a ZF as annotated. The optical spectrum of the isolated mitoNEET exhibited absorbances centered at 458 nm and 530 nm [57]. These absorption peaks are indicative of a [2Fe-2S] cluster, and are observed in established [2Fe-2S]

cluster co-factored proteins such as ferredoxin (CCCC ligand set) and Rieske (CCHH ligand set) proteins [57]. While this biochemical characterization of mitoNEET was in progress, studies in COS-7 cells (a primate cell line) revealed that mitoNEET associates to the outer mitochondrial matrix with the CCCH domain facing towards the cytoplasm. This is associated with the protein's ability to regulate the oxidative capacity of the mitochondria suggesting a potential redox role [69]. Taken together, the iron stoichiometry, the optical spectrum, and the association of mitoNEET with oxidative capacity of the mitochondria, led the Dixon and Jennings laboratories, to propose that the co-factor of mitoNEET was an Fe-S cluster and suggested a role in regulation via redox chemistry [57, 69].

To determine if the Fe-S cluster of mitoNEET could support redox chemistry, the protein was treated with the reductant dithionite. This treatment resulted in a loss of the absorbance peak centered at 458 nm indicative of reduction of one of the ferric centers [57]. Addition of oxygen reversed this signal loss, indicating redox cycling at the Fe-S cluster. This work supports a role for mitoNEET in redox sensing [57]. To confirm redox activity, electron paramagnetic resonance (EPR) spectra of the reduced and oxidized mitoNEET proteins were obtained. The spectrum of the oxidized protein showed no signal, as expected for the Fe(III)-Fe(III) species; while the reduced protein exhibited a rhombic signal which is consistent with an Fe(II)-Fe(III) species [57]. Native mass spectrometry which reports on the folded, metal-bound protein was utilized to determine metal stoichiometry. Mass shifts corresponding to the presence of a singular [2Fe-2S] cluster were present [57].

To identify the ligands for this new Fe-S cluster, the amino acids that are conserved in mitoNEET, Miner1 and Miner2 - Cys-72, Cys-74, Cys-83, His-87, and Asp-84 – were systematically mutated with serine (for cysteine), glutamine (for histidine) and asparagine (for aspartate). The effects of the mutations were measured by UV-visible spectroscopy and a loss of signal for the Fe-S cluster was observed in all of the mutants except the D84N mutation. These data offer support for the CCCH ligand set. This was the first time that a native [2Fe-2S] cluster co-factored protein was observed to contain a CCCH ligand set instead of a CCCC or CCHH ligand set. MitoNEET is also pH sensitive; the optical spectrum of the WT protein lost signal upon lowering the pH, which was not observed in the CCCC mutant. This was attributed to the sole histidine ligand, which is likely protonated when the pH is lowered, leading to the dissociation of the cluster and the inactivation of the protein [57].

The CCCH domain present in mitoNEET and related homologs has been further classed as a CDGSH domain to reflect the conservation of additional amino acids. Notably, this domain is conserved from bacteria to humans, suggesting that the site may have been present in a pre-oxygen time period [57]. As organisms evolved to survive in an oxygen rich environment, this site may have been retained to fulfill an important function.

This seminal work on mitoNEET came forty years after the discovery of the now well-established Ferredoxin (CCCC) and Rieske (CCHH) type Fe-S cluster proteins (**Figure 3**). The identification of a third type of [2Fe-2S] cluster has resulted in a surge in research on mitoNEET itself. Advances have been made in understanding the protein's roles in redox control as well as the

role of the protein in disease [68, 70-82]. Altogether, the work on mitoNEET underscores the need to empirically define metal co-factors and to not solely rely on bioinformatic annotations.

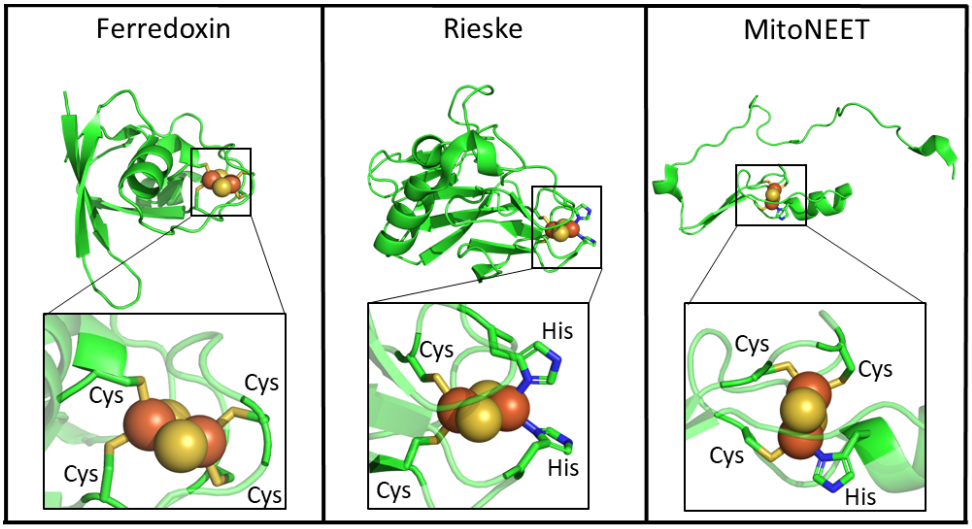

Figure 3. The structures of ferredoxin, Rieske, and mitoNEET, with a focus on the [2Fe-2S] clusters and associated ligands. Ferredoxin (PDB: 5AUI) utilizes 4 cysteines as ligands. Rieske (PDB: 2NVF) type Fe-S clusters contain 2 cysteine and 2 histidine ligands. MitoNEET (PDB: 2R13) contains 3 cysteine and 1 histidine ligands.

3. Case study #2: CPSF30

Cleavage and polyadenylation specificity factor 30 (CPSF30) is a protein involved in pre-mRNA processing [54, 83-87] (**Figure 4A**). Pre-mRNA processing is an important step in eukaryotic gene expression and subsequent protein translation to maintain cellular homeostasis. A key step in pre-mRNA processing is the 3' end maturation step. Here, the pre-mRNA is cleaved, and poly(A) polymerase is recruited to add an elongated poly adenosine (poly A) motif resulting in mature mRNA (**Figure 4B**). Defects in polyadenylation are associated with several disease states including α/β thalassemia, lupus, and fabry disease [88-95]. Due to the processes' essential

role in alternative polyadenylation, gene regulation, disease, and maintenance of cellular health, pre-mRNA processing is of high importance for fundamental research and as a therapeutic target.

A main protein complex that regulates pre-mRNA processing is the cleavage and polyadenylation specificity factor (CPSF) complex. CPSF is composed of 6 different proteins that participate in the recognition of the highly conserved polyadenylation signal (PAS) AAUAAA, cleavage of the 3' end of pre-mRNA, and the recruitment of additional polyadenylation machinery (**Figure 4B**). Our laboratory, which has a research program focused on 'CCCH' type ZF proteins, became interested in studying CPSF30 because it contained five CCCH domains. We had previously investigated another 'CCCH' type ZF called tristetraprolin (TTP or Nup475), and demonstrated that when it is bound to zinc, it recognizes AU rich RNA [96, 97]. CPSF30 is part of a complex that recognizes an AU rich target (AAUAAA), therefore we hypothesized that CPSF30 was the protein responsible for binding this target. However, when we isolated and purified a construct of CPSF30 that contained all five CCCH domains using a standard ZF approach that involved expressing the protein, purifying in the apo-form, and titrating with zinc to fold, the protein was found to be highly insoluble. MBP fusions are often utilized to increase recombinantly expressed protein solubility. This method has been utilized successfully for many ZFs and metalloproteins as well as mitoNEET [57, 69]. This fusion approach was also pursued for CPSF30 [54, 98-101]. Remarkably, when the fusion construct was expressed, the cell pellet turned a brownish red color (MBP alone does not show this color). This color persisted upon purification, and the optical spectrum of the purified holo-protein

exhibited peaks centered at 420 nm, 456 nm, and 583 nm which are suggestive of a [2Fe-2S] cluster, much like what was observed for mitoNEET [54, 102]. X-ray absorption spectroscopy (XAS) and inductively coupled plasma mass spectrometry (ICP-MS) were then conducted to verify this prediction of a [2Fe-2S] cluster. ICP-MS revealed that 0.51 and 3.78 equivalents of Fe and Zn were present per protein, respectively [54]. XAS showed that Zn was bound tetrahedrally by a CCCH ligand set similar to other ZF domains and the presence of a [2Fe-2S] cluster was observed bound by a CCCH ligand set as well. The [2Fe-2S] cofactor was identified to have an Fe-Fe vector of 2.67 Å, a Fe-S length of 2.26 Å (average), and a Fe-N (or O) length of 2.03 Å, consistent with bond lengths reported for other [2Fe-2S] clusters [103]. Once we had identified the metal co-factors of CPSF30, functional assays using fluorescence anisotropy (FA) were performed. We determined that Zn/[2Fe-2S] cluster loaded CPSF30 selectively recognized the AAUAAA motif, as predicted. Chelation studies showed that both metals were needed for full binding affinity, underscoring the importance of the iron sulfur cluster in CPSF30 function [54]. Mutagenesis studies to locate the site of the Fe-S cluster revealed flexibility in site loading. In these studies, each CCCH domain was sequentially mutated to AAAA, and the proteins were isolated and metal content assessed by ICP-MS. Iron was present in all of the mutant proteins, suggesting that CPSF30 has redundant sites for iron binding, and that the cluster can be loaded in another site when the “preferred” site is mutated [54]. We proposed that the essential role of CPSF30 in pre-mRNA processing requires this built-in redundancy. These data added CPSF30 to the growing list of proteins that were annotated as ZF proteins but were found to harbor a

[2Fe-2S] cluster co-factor. The role of the Fe-S cluster in mammalian CPSF30 remains under study. Notably, CPSF30 been shown to associate with HSC20, which is the eukaryotic (human) Fe-S chaperone protein suggesting a source for the Fe-S co-factor. In addition, regulation of redox control mechanisms have been observed in some CPSF30 homologs. The yeast homolog, YTH1, has been observed to translocate from the nucleus to the cytoplasm under hypoxic stress mediated by an unknown mechanism [104]. Additionally, the *Arabidopsis thaliana* homolog is known to be regulated under oxidative stress mediated by a disulfide bond forming in one of its ZF domains [105-107]. Therefore, the Fe-S cluster cofactor may be required by the mammalian CPSF30 homolog for oxidative stress sensing and regulation.

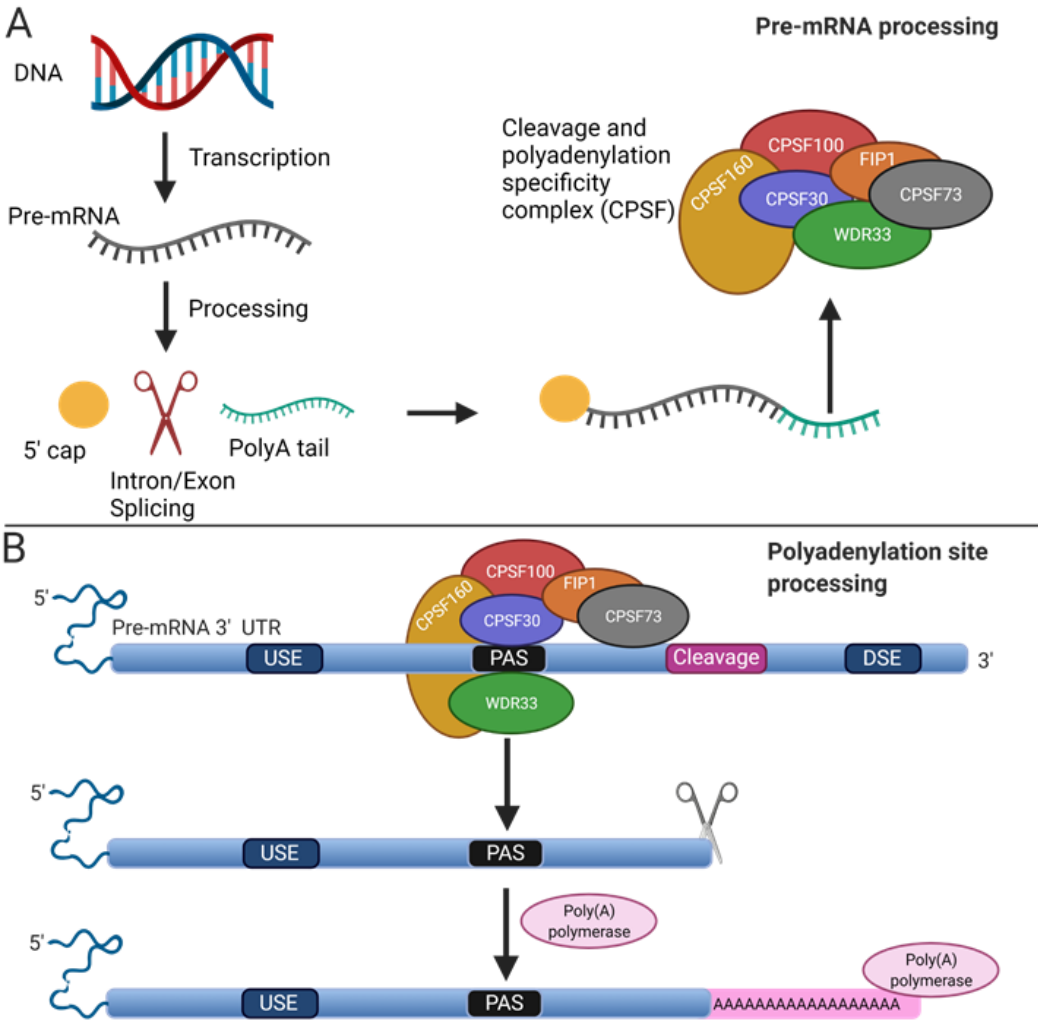

Figure 4. Overview of pre-mRNA processing and the role of CPSF30. (A) General overview of pre-mRNA processing. DNA is transcribed into pre-mRNA, processed in to mature mRNA where a 5' cap is added, introns and exons are then spliced, and a polyA tail is added. (B) An overview of the role of CPSF30 in pre-mRNA site selection mediated by the CPSF complex. Reprinted (adapted) with permission from *Biochemistry* 2021, 60, 10, 780-790. Copyright 2021 American Chemical Society.

4. Case study #3: nsp12

In 2020, the severe acute respiratory syndrome coronavirus 2 (SARS-CoV-2 which leads to the disease COVID-19) spread rapidly causing a global pandemic. Although vaccines with high efficacy for SARS-CoV-2 have been developed, small molecule drugs to inhibit the virus are still needed [55]. Such drugs can protect from breakthrough infections and target new variants for which vaccines are not yet available [55]. RNA-dependent RNA polymerase (RdRp) plays an integral role in the synthesis of viral RNA and subsequently the life cycle and virulence of SARS-CoV-2, making it a prime drug target [55]. RdRp is a complex of proteins comprised of a main cofactor nsp12 and accessory factors nsp7 and nsp8. Nsp12 was predicted to contain two ZF domains. This prediction was based upon primary sequence analysis and modeling studies of a SARS-CoV homolog which had 2 ZFs (HCCC and CHCC) [55]. Cryo-EM structures of nsp12 alone and nsp12 with nsp7 and nsp8 modeled zinc in these sites as a co-factor [108-111] (**Figure 5**). The Rouault laboratory sought to characterize the nsp12, nsp7 and nsp8 protein complex to determine its suitability as a druggable target. While investigating this complex, they made the interesting discovery that the 'ZF' co-factors are Fe-S clusters [55].

The Rouault laboratory had previously identified a specific LYR motif that is present in proteins to which the Fe-S cluster chaperone HSC20 protein transfers its cluster [58-61]. They proposed that this motif is a general sequence 'signal' associated with proteins that harbor an Fe-S cluster. Nsp12 has 2 LYR-like motifs (VYR and LYR) within its primary sequence suggesting it can accept an Fe-S cluster from HSC20. Rouault and co-workers,

teamed up with the Bollinger and Krebs laboratories and demonstrated that purified nsp12 and HSC20 exhibit a strong binding interaction, and that when the LYR motif was mutated to AAA, the binding interaction was abrogated. The finding of the nsp12/HSC20 protein-protein interaction supported the hypothesis that nsp12 can accept an Fe-S cluster and requires the 'LYR' motif signal sequence. Subsequent coimmunoprecipitation (Co-IP) studies in mammalian cells confirmed the nsp12/HSC20 interaction and also revealed that nsp12 associated with other parts of the Fe-S cluster machinery. Together, these data suggest that nsp12 is an Fe-S cluster protein instead of a ZF.

To directly confirm that nsp12 has an Fe-S cluster co-factor, the protein was expressed in mammalian cells grown with ^{55}Fe [55]. Upon purification the Fe incorporation into nsp12 was measured via scintillation counting and significant iron incorporation was observed. The optical spectrum of the isolated nsp12 included an absorbance centered at 420 nm, suggesting that the iron was incorporated as an Fe-S cluster [58, 63]. When the LYR motifs were mutated, less Fe was incorporated and when ISCU (an important protein in Fe-S cluster synthesis) was downregulated, no iron was detected bound to nsp12. Subsequent Mössbauer spectroscopy revealed that the cluster is a [4Fe-4S] cluster. Altogether, this work on the 'ZF' protein nsp12 revealed that it binds two [4Fe-4S] clusters in previously annotated metal binding sites.

The functional significance of the Fe-S cofactor in nsp12 function was determined using an RNA elongation assay. This assay measures the activity of RNA polymerase. When the protein was loaded with the Fe-S cluster, significant elongation was measured. However, the Zn loaded protein

exhibited lower activity. These data support a role for the Fe-S co-factor in nsp12 function.

The overarching goal of this work was to determine if nsp12 is a drug target. As such, the effect of TEMPOL on activity was investigated. TEMPOL is a stable nitroxide that has been shown in animal models to disassemble Fe-S clusters [112, 113]. The hypothesis was that if TEMPOL targeted nsp12 at its Fe-S cluster, it would lower RdRp activity and diminish virulence. Rouault and co-workers determined that TEMPOL disassembled the Fe-S cluster in nsp12. Moreover, little to no cytotoxicity was observed in mammalian cell cultures, suggesting it may be a viable lead for drug screening. TEMPOL was found to have high activity towards inhibition of SARS-CoV-2 replication and synergized with remdesivir, which is used to treat COVID-19 [55]. Together, these findings provide another example of the importance of empirically determining the co-factor in annotated ‘ZFs’ [55].

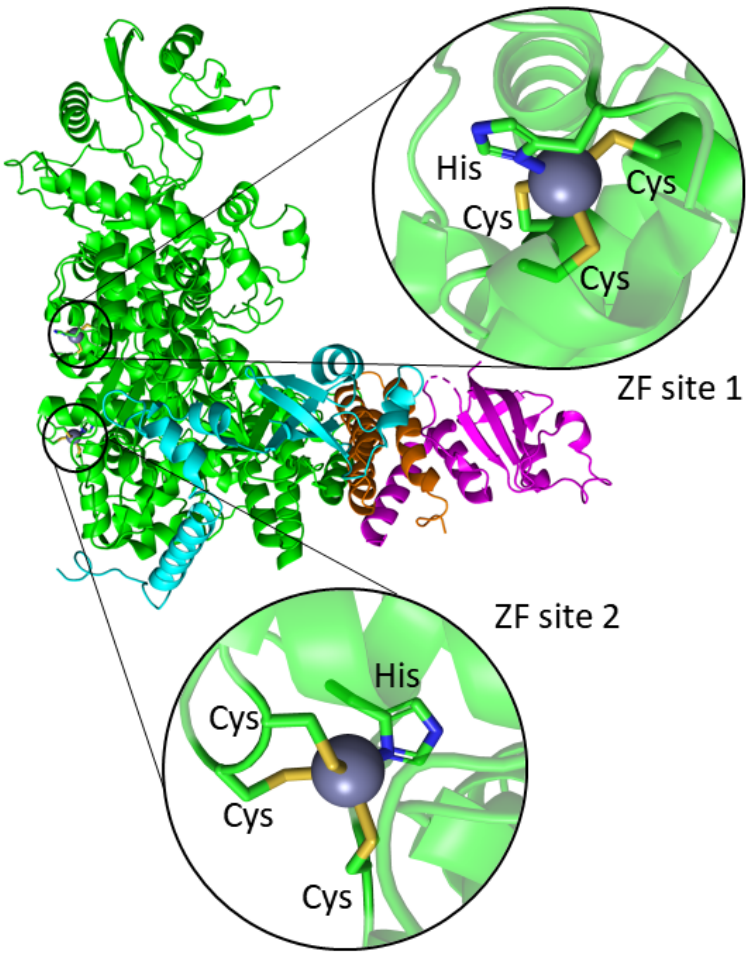

Figure 5. Cryo-EM structure of RdRp with the nsp12 metal binding sites modeled with zinc. Nsp12 is shown in green, nsp7 is shown in orange and 2 monomers of nsp8 are shown in cyan and magenta. Zoom in of the annotated 'ZF' sites of nsp12 are shown with 3 cys and 1 his ligands. The RdRp structure was obtained from the PDB (7BTF) and modeled in Pymol.

5. Case study #4: Fep1

Iron-sensing transcriptional repressor (Fep1) is part of a family of regulatory proteins referred to as GATA factors. GATA factors bind and regulate 5'-(A/T)GATAA-3' sequences in yeast and fungi [56]. These proteins contain two canonical CCCC ZF domains (Cys-X_2-Cys-X_{17-18}-Cys-X_2-Cys) as well as a non-canonical CCCC ZF domain (Cys-X_5-Cys-X_8-Cys-X_2-Cys)

located between the two canonical domains [56, 66]. The function of the Fep1 protein is to sense and regulate Fe, but its complete mechanism has not been determined. It is not known whether the sensing mechanism involves direct iron binding to the protein. Interestingly, SRE-1, a GATA homolog from *Histoplasma capsulatum*, was isolated with iron present, suggesting a potential role for an iron co-factor [56, 114]. These findings led Bonaccorsi di Patti and co-workers to hypothesize that *Pichia pastoris* Fep1 may also bind iron directly. Studies in cells that compared the iron sensing capabilities of WT Fep1 protein versus mutant Fep1 proteins in which the non-canonical CCCC domain had been modified, showed that iron sensing was disrupted when the non-canonical CCCC domain was mutated. This suggested that this domain may serve as the site of iron binding. Fep1 protein was then isolated *in vitro* and was observed to be a reddish color and contain iron (via ICP-AES) offering further evidence that Fep1 has an Fe co-factor.

Subsequent mutagenesis studies of Fep1 revealed that the iron recognition is complex. A series of mutants, starting with the non-canonical CCCC domain modified to SSSS (4S) were prepared and the effects on iron binding were evaluated. When the non-canonical domain was knocked out (4S), the protein was still brownish-red upon purification, like WT. This indicated the presence of an Fe binding domain. UV-visible absorption spectra of the 4S mutant exhibited peaks centered around 410, 325, and 455 nm, which are indicative of an Fe-S cluster, and which are similar to but not identical to those observed for WT Fep1 (peaks centered at 413, 325, 455 nm). Resonance Raman data collected for the mutant and WT constructs were consistent with the Fe-S cluster binding to a CCCC ligand site in both cases.

Together, these data suggest that the Fe-S cluster is loading elsewhere when its presumed binding site is mutated. The only other cysteine ligands present in the Fep1 sequence are those that make up the two canonical CCCC ZF domains. This suggests these may be the sites of iron binding. Bonaccorsi di Patti and co-workers proposed that one or more of these ZF domains serve as 'rescue sites' for the [2Fe-2S] cluster.

The 'rescue site' hypothesis was then tested via a series of mutants in which each of the two canonical CCCC ZF domains (ZF1 and ZF2) were modified. ZF1 could 'rescue' the Fe-S site, whereas, Fe-S binding to ZF2 was never observed in any mutants. The effect of oxygen on iron loading was also investigated with a series of mutants. It was discovered that under aerobic conditions, the Fe-S cluster was not air stable in the non-canonical site and instead bound to a new site made up of two C ligands from the non-canonical ZF site and two C ligands from the canonical ZF1 site (**Figure 6**). Additionally, in the anaerobically purified protein, the Fe-S cluster was present at the non-canonical site. This finding connects with the biological function of the protein, which is an oxygen and iron sensor [56]. As with the other misannotated ZFs, the experimental data collected for Fep1 underscore the importance of verifying ZF sites.

This is not the first time that Fe-S cluster redundancy has been observed. Similar redundancy was reported for the mutants of CPSF30. When specific CCCH ZFs in CPSF30 are mutated to AAAA, iron is still detected suggesting that the Fe-S cluster is loaded at an alternate CCCH site when the "preferred" site is compromised. This may be a mechanism for regulating Fe-S cluster protein activity or it may provide an auxiliary site to prevent full loss of

activity under conditions such as stress.

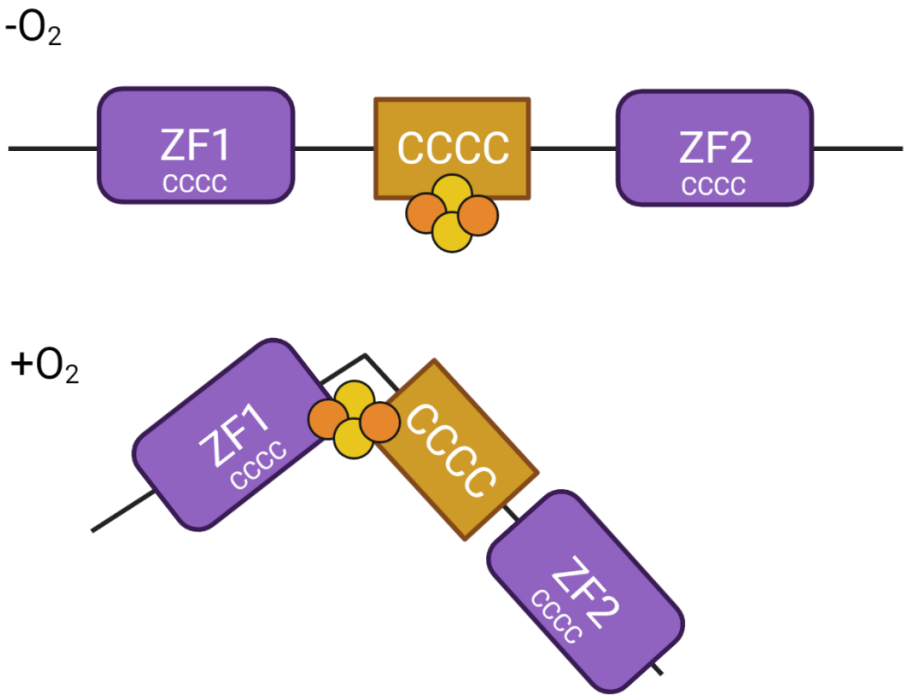

Figure 6. Cartoon diagram of the three CCCC domains present in Fep1 with the sites of Fe-S binding under anaerobic and aerobic conditions shown at the top and bottom respectively.

6. Lessons learned from studying annotated ZFs

Although ZF proteins are ubiquitous in eukaryotes, many are only known at the sequence level and/or have been characterized in cells and have been presumed to be ZFs based upon their sequence. Ideally, one should be able to study a ZF in vitro and in vivo, and directly correlate the data obtained; however, this remains a challenge [115]. We can isolate individual ZF proteins to determine their metal co-factors and identify macromolecular targets in vitro. We can also study ZF protein activity in cells and detect responses to changes in other proteins or global metal levels, but we do not yet have the technology to directly measure metalation of single ZFs in cells. As such, one

must take in vitro data along with indirect cellular data to draw conclusions about the metal:protein pairing in vivo. As such, the conclusions that we draw from these studies may not be the complete story in vivo. With advances in cell biology methods and the increased sensitivity of analytical instrumentation, we may be able to better correlate these data in the future. With this caveat in mind, direct analysis of isolated proteins in vitro coupled with cellular data can be informative, as is described in this focused review. The biochemical data of the four annotated ZFs, mitoNEET, CPSF30, Fep1 and nsp12, revealed that these specific 'ZF' proteins are isolated with Fe-S co-factors. Cellular data were then utilized to correlate these in vitro findings with potential biological roles: the Fe-S cluster of mitoNEET regulates the oxidative capacity of the mitochondria via a redox change, CPSF30 associates with the Fe-S chaperone HSC20 and its homologs are involved in regulation of oxidative stress, the Fe-S cluster in nsp12 promotes RNA elongation as part of the RNA dependent RNA polymerase (RdRp) and Fep1 plays a role in iron/oxygen sensing [55, 56, 61, 69, 104-107].

As well as the importance of considering in vitro results in terms of a protein's in vivo role, there are additional hurdles that accompany isolating proteins in vitro and identifying the metal co-factor that must be considered. Ideally, proteins should be isolated in their native hosts; however, this can be prohibitively difficult as metal analysis and protein characterization requires higher concentrations of the protein than are present under native conditions. This is especially true for eukaryotic proteins, such as ZFs, which can be present at very low concentrations in cells [116, 117]. Thus, isolation of metalloproteins typically relies on the over-expression of the protein in a host

cell to obtain sufficient yields for analysis. Overexpression of proteins can affect metal loading because the protein is being produced at higher levels in the cell than the native proteins. Moreover, overexpression often requires a heterologous expression system, especially for eukaryotic proteins, and this can lead to mismetallation because the native protein loading machinery is not present [115]. One approach to favor correct metal loading is to incorporate the proteins that are involved in metal assembly in the native host in the over-expression system. For instance, the ISCU system which promotes Fe-S cluster assembly in eukaryotic proteins has been utilized with success in some instances [118-120]. However, the machinery for metal incorporation is not always known and/or does not always impact metal loading [56, 57]. If the function of the protein has been determined, e.g., it is an enzyme that catalyzes a specific reaction or it is a transcription factor that binds to a specific DNA target, studying the protein's function in the context of its metal co-factor can provide data that supports the in vitro metal co-factor assignment. Here too, a limitation is that the function of the protein may not be known, or the protein may be active with more than one type of metal co-factor. Taken together, an approach in which in vitro characterization is one puzzle piece that is correlated with other puzzle pieces - cellular and biological data – allows for a more comprehensive understanding of the protein of interest.

7.0. Experimental approaches to characterize newly isolated ZF proteins

In the next section, we present a primer on methods that are useful for the characterization of ZF proteins in vitro, including those with potential 'Fe-S' co-factors. While those in the field may be intimately involved in these methods, this primer is intended to provide guidance for those who do not work in this area.

7.1. Common Ligands for ZFs and Fe-S Centers

Metalloproteins commonly utilize amino acids that have sulfur, oxygen and nitrogen as ligands [30, 121]. Cysteine, histidine, glutamate and aspartate are the most frequently utilized ligands, although serine, tyrosine, threonine, glutamine and asparagine have also been identified in a small number of proteins [121]. Proteins with zinc (ZFs) and iron-sulfur cluster co-factors both utilize cysteine and histidine residues as metal binding ligands, often using identical sequence motifs (e.g CX_2C). This can make it challenging to predict whether a newly identified protein will coordinate zinc or an Fe-S cofactor. This challenge was underscored in a recent study that aimed to identify metalloprotein co-factors using 'sequence patterns' rather than sequence motifs. In this study, the wealth of structural information available for metalloproteins in the PDB was utilized to develop a tool, called pattern discovery in PDB structures of metalloproteins (PdPDB). This tool considers the complete coordination sphere, including contributions from nucleic acids and small molecule ligands to define the 'sequence pattern' and the metal binding ligands identified in the PDB structures (e.g., sulfur from cysteine) are prioritized in the analysis. From PdPDB, ligand patterns for each type of Fe-S

cluster, as well as for mononuclear Fe sites, structural Zn sites (ZFs), and hydrolytic Zn and Mg sites were identified. The patterns were then compared, using Pearson correlation coefficients, and plotted to identify similarities and differences. As shown in **Figure 7**, if two types of sites have a strong Pearson correlation, the correlation is indicted by a dark blue box and has a score close to or equal to 1. If two types of sites have low correlations, the box is a lighter blue or white with a correlation coefficient closer to 0. Notably, mononuclear Zn sites (e.g., ZFs) showed a strong correlation with Fe-S sites – both 2Fe-2S and 4Fe-4S, as did mononuclear rubredoxin, whereas limited correlations were observed between hydrolytic sites with Zn, Fe^{+2}/Fe^{+3} or Mg. This finding revealed that much like using sequence motifs, there are strong similarities between ZF sites and Fe-S sites in metalloproteins [62].

The structural, electronic, and vibrational environment of a metal center can be reflective of oxidation state, metal and ligand identity, and stoichiometry [30, 122-124]. Common spectroscopic and analytical techniques utilized to characterize these metal centers include UV-visible spectroscopy (UV-vis), inductively coupled plasma mass spectrometry (ICP-MS), X-ray absorption spectroscopy (XAS), Electron paramagnetic resonance spectroscopy (EPR), Mössbauer spectroscopy, resonance Raman spectroscopy (RR), circular dichroism (CD), and native electrospray ionization mass spectrometry (ESI-MS). When studying new metalloproteins, these techniques are often coupled with mutagenesis to allow for the identification of coordinating ligands. No singular technique is sufficient to fully characterize a metal center so a suite of studies are necessary. Here we focus on methods that are relevant to Zn and Fe-S sites, some of which have been pursued in the

'cases' described in this review and our laboratory [41, 45, 54-57, 69, 85, 86, 96, 102, 125-130].

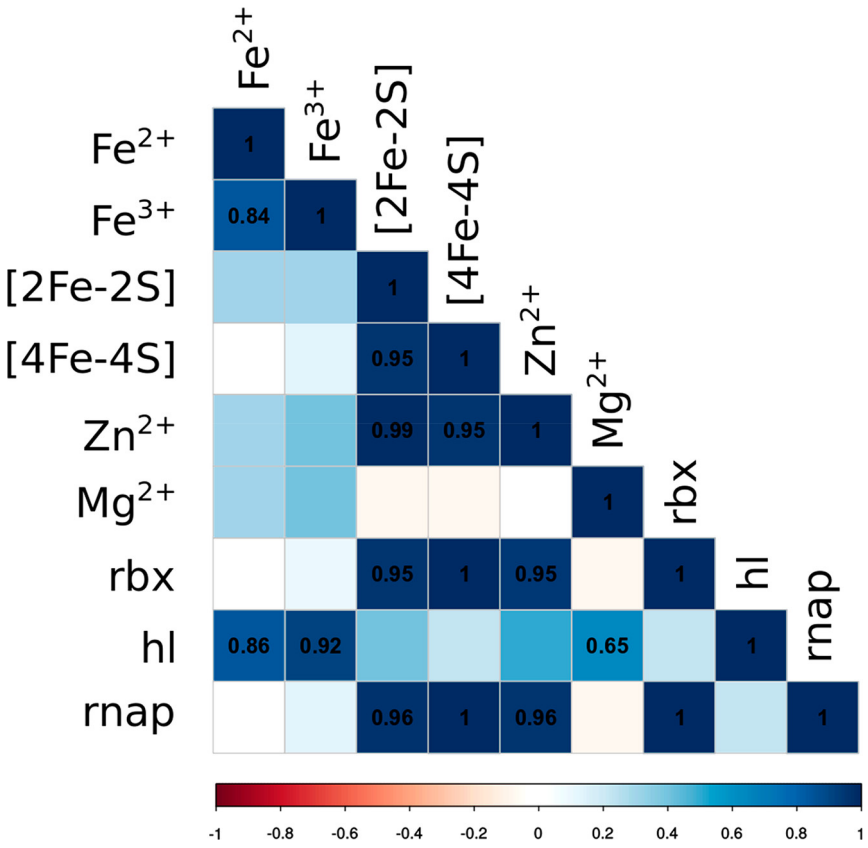

Figure 7. The correlation scores of ligand patterns determined for metal cofactors using PdPDB [62]. Enrichment scores of ligand distribution were used to calculate Pearson correlation coefficients. Larger coefficients indicate a stronger correlation and are shown as dark blue. White indicates no correlation and red indicates negative correlations. Rubredoxin (rbx – a tetrahedral Fe site), hydrolase (hl – a catalytic Zn site) and RNA polymerase (rnap – a structural zinc site) are also shown. Reprinted (adapted) with permission from *J. Chem. Inf. Model.* 2017, 57, 12, 3162-3171, https://pubs.acs.org/doi/10.1021/acs.jcim.7b00468. Notice to readers: Further permissions for this excerpted material should be directed to the ACS.

7.2. Apo protein metal binding vs holo protein isolation

Zinc finger proteins are often studied in the apo form (metal-free); this is accomplished via either peptide synthesis of constructs that consist of ZF domains or via purification of expressed proteins under denaturing conditions [40, 50, 97, 131-133]. The apo-ZF domains can then be folded around zinc in

vitro via direct addition of a zinc salt (e.g., $ZnCl_2$) under buffered conditions (**Figure 8**). Although this method is very useful, it assumes that the annotated ZF is a *bona fide* zinc binding protein. Per the Irving-Williams series, the apo-ZF will show a thermodynamic preference for zinc over most other transition metals, including iron *(vide infra)* therefore in this approach zinc will preferentially bind as the co-factor. Metal coordination in the cell is not always thermodynamically driven, and metal availability can influence metal binding leading to mis-assignment of metal cofactors [2, 3, 55, 134]. Another approach to identify the metal co-factor for a ZF protein is to express and purify the protein in the holo-form (metal bound) [54, 135]. This allows for isolation of the protein with its endogenous metal(s) bound. Our laboratory's work on CPSF30, a protein that was annotated as a ZF (*vide supra)* provides an example of this approach. When CPSF30 was isolated in the apo-form addition of zinc did not result in a folded, soluble protein, despite various approaches to refold. In contrast, when CPSF30 was isolated in the holo-form, the protein was readily soluble, and led to the discovery that one of the ZF sites contained an Fe-S cluster. Additionally, isolation of proteins in the holo form allows for proteins to be expressed with solubility tags, which can also aid in characterization.

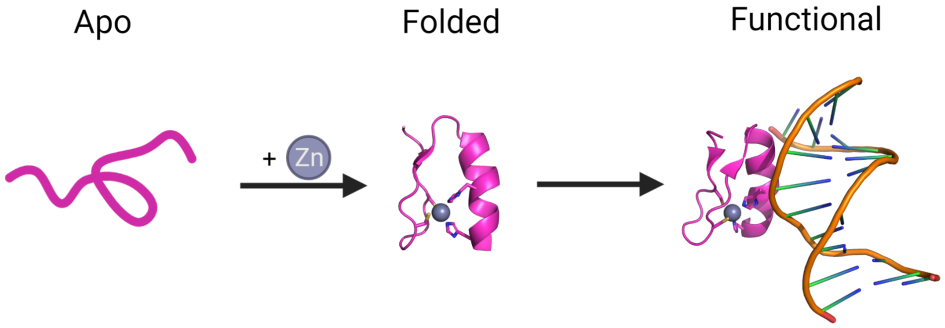

Figure 8. Cartoon diagram of the ZF paradigm using the classical ZF ZIF268 as an example. In the apo form, the ZF is unfolded, upon addition of Zn, the ZF adopts secondary structure that allows for function (e.g., DNA, RNA, or protein binding). Note: More than 1 ZF is usually needed to recognize its binding partner. (PDB 1A1L)

7.3. UV-Visible spectroscopy (Fe-S cluster and Co/Zn titrations)

UV-Visible spectroscopy is a ubiquitous technique in biochemistry and bioinorganic chemistry laboratories. It is commonly used to determine protein concentrations, because theoretical extinction coefficients for proteins that contain tryptophan, phenylalanine, and tyrosine can be calculated [136]. These extinction coefficients can then be used to convert measured absorbance to concentration via Beer's law [123, 137]. When metals are present as co-factors, additional optical bands can be observed. These include ligand-to-metal charge transfer, metal-to-ligand charge transfer, and d-d transitions. Electronic absorption spectra for these types of transitions can be found in the ultraviolet, visible, and near infrared regions [30, 138]. These unique metal centered absorbances can be integral to characterizing metal sites. Iron-sulfur clusters often show distinct absorbances in the 400-600 nm range, with 2Fe-2S clusters exhibiting a characteristic peak maximum centered between 410-430 nm [63] (**Figure 9A-B**). The basis of these absorption spectra is complex. It

took 20 years from the identification of the first Fe-S cluster from succinic DPNH dehydrogenase using EPR by Beinert and Sands for the UV-Vis absorbance bands to be assigned as the cysteine to Fe charge transfer excitation, by Noodleman and coworkers [139-142]. Around the same time, Aizman and Case assigned the absorbance observed in the visible range to both d-d and ligand to metal charge transfer transitions [143]. The complexity of the electronic structure of 2Fe-2S clusters is due, in part, to the antiferromagnetic coupling between the two iron centers, and the 'non-innocent' sulfur atoms in which there is a high degree of electron delocalization from the sulfur atoms, contributing to high covalency of the Fe-S bonds. Recent work has suggested a re-assignment of the optical spectra of 2Fe-2S centers. Kubas calculated the electronic structure of - $[Fe_2S_2](SMe)^{2-}_4$ which is closely related to a 2Fe-2S cluster model complex ($[Fe_2S_2](SEt)^{2-}_4$) that had been previously reported by Holm and co-workers [144, 145]. The calculated structure has absorbance bands that match those measured experimentally by Holm and co-workers [144, 145]. Notably, in Kubas' calculated structure, the absorbance for the 2Fe-2S cluster that is observed at 400 nm is attributed to a charge transfer excitation between the bridging μ-sulfur atom to Fe(III), instead of cysteine to Fe(III) charge transfer as previously assigned [144, 145]. Regardless of the assignment of the bands, 2Fe-2S clusters exhibit unique optical spectra that can aid in the identification of newly isolated proteins. Additionally, the Fe-S charge transfer bands are sensitive to changes in redox state and exogenous ligand binding (e.g., NO), and therefore UV-visible spectroscopy can be used to monitor these changes. Once changes are observed by UV-visible spectroscopy, additional

spectroscopic methods can then be utilized to confirm and further characterize the changes at the iron center.

Optical spectroscopy is also commonly used to characterize ZFs. Although Zn(II) is spectroscopically silent because it is d^{10}, Co(II) can be used as a spectroscopic probe [146]. Cobalt readily binds to cysteine and histidine ligands in the ZF site in a tetrahedral geometry, like Zn. However, Co(II) has the advantage of having an unfilled d shell (d^7) and when ligands are coordinated in a tetrahedral geometry, distinct d-d transition bands in the 550-750 nm range are observed (**Figure 9C**) [85]. Co(II) binds more weakly than Zn(II), because of ligand field stabilization energy differences, therefore Zn(II) affinities can be determined via competitive Co/Zn titrations [147]. In these experiments, first Co(II) is titrated with the apo-ZF and the changes in the d-d bands are observed (**Figure 9C**) [85]. Subsequently, Zn is then titrated with the Co-ZF, and the data are fit to a competitive binding model and upper limit K_ds can be determined (**Figure 9E-F**) [85]. Zn typically binds in the nanomolar to picomolar region (K_d), therefore only an upper limit K_d can be reported due to the sensitivity of UV-visible spectrometers. UV-Visible spectroscopy is a workhorse technique due to its versatility and ease of use.

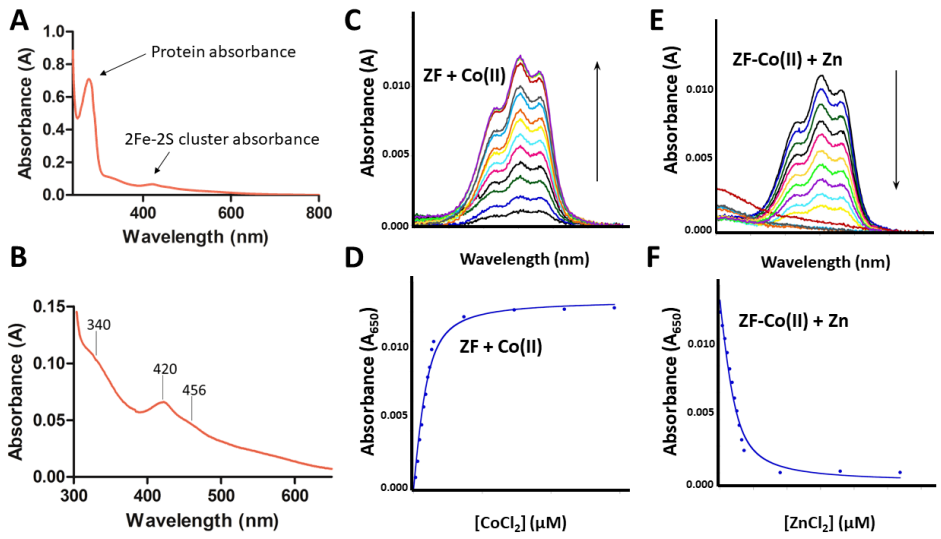

Figure 9. The optical spectra of the [2Fe-2S] cluster of CPSF30 the Co/Zn spectra for F2+F3 of CPSF30 adapted from reference [85]. The full optical spectrum of CPSF30 is shown in (A). A focused optical spectrum of the Fe-S center of CPSF30, between 300-650 nm is shown in (B). A titration of CPSF30 ZF2+ZF3 with cobalt is shown in (C) and its fit to a 1:1 Binding equilibrium is shown in (D). A titration of Zn with Co-CPSF30(ZF2+ZF3) is shown in (E) and its fit to a competitive binding model is shown in panel (F). For A-B the buffer was 20 mM Tris, 100 mM NaCl, at pH 8. For figures C-F the buffer was 200 mM HEPES, 100 mM NaCl at a pH of 7.5. Reprinted (adapted) with permission from *Biochemistry* 2020, 59, 8, 970-982. Copyright 2020 American Chemical Society.

7.4. ICP-MS (or AES)

Inductively coupled plasma mass spectrometry or atomic emission spectroscopy **(**ICP-MS or ICP-AES) are techniques that quantify elements in a system such as a protein, tissue, or cell. This technique is extremely sensitive and allows for element detection down to parts per trillion. For proteins of known concentration, the metal to protein stoichiometry and metal identity can be determined. ICP-MS is an excellent complement to techniques such as UV-Visible spectroscopy, XAS, Mössbauer, EPR, and resonance Raman to characterize metal identity, stoichiometry, ligands, and oxidation state. For

more in depth information on ICP-MS and AES of metalloproteins we direct you to these helpful reviews [102, 148-151].

7.5. XAS

X-ray absorption spectroscopy (XAS) is a solution-based technique that utilizes X-rays to probe metal sites. In this experiment, which is conducted at a synchrotron, high energy X-rays cause electrons from core orbitals (e.g., S), to be excited. The resultant data provides an indication of metal, oxidation state, geometry, coordination number, and ligands. The XAS data has three regions of interest: pre-edge, XANES, and EXAFS [152, 153]. As shown in **figure 10** for CPSF30 which has both a 2Fe-2S co-factor and a Zn co-factor, specific differences can be observed in XAS obtained for Fe-S clusters versus ZFs. The Fe and Zn excite at different energy levels (~7111-7150 eV and 9657-9682 eV respectively) which allows for metal identification. In **figure 10A** the pre-edge of the Fe XANES centered at ~7112.4 eV shows a 1s-3d transition indicating the presence of a 4-coordinate tetrahedral ferric iron site. In the rising edge of the Fe XANES (**Figure 10A**), an inflection point at 7120 eV is observed indicating the presence of an oxidized 2Fe-2S (Fe(III)-Fe(III)) cluster (**Figure 10A**) [54]. The Fe EXAFS in **figure 10B** and **C** are best fit to 3 Fe-S bonds, with an average bond length of 2.26 Å, 1 O/N bond with a bond length of 2.03 Å, and an Fe-Fe vector at 2.67 Å. These data were in line with expected values for 2Fe-2S clusters bound to 3Cys and 1His residues. The XANES data for Zn are given in **figure 10D**. Since Zn has a completely filled d orbital, no pre-edge data are observed. However, it can be determined that Zn is present as Zn^{2+} by the half-height of

the normalized fluorescence at 9662.5 eV. In the post-edge region, the intensities at 9665.7 eV and 9671 eV are indicative of Zn-S and Zn-O/N bonds. The EXAFS data in **figure 10E** and **F** are best fit to 1 O/N bond at a distance of 2.01 Å and 2.5 S bonds at an average distance of 2.31 Å. Together, these data are similar to Zn bound peptides containing 3Cys and 1His residues [54]. For more in depth information on XAS of metalloproteins we would like to refer the reader to these helpful reviews [102, 152, 154-157].

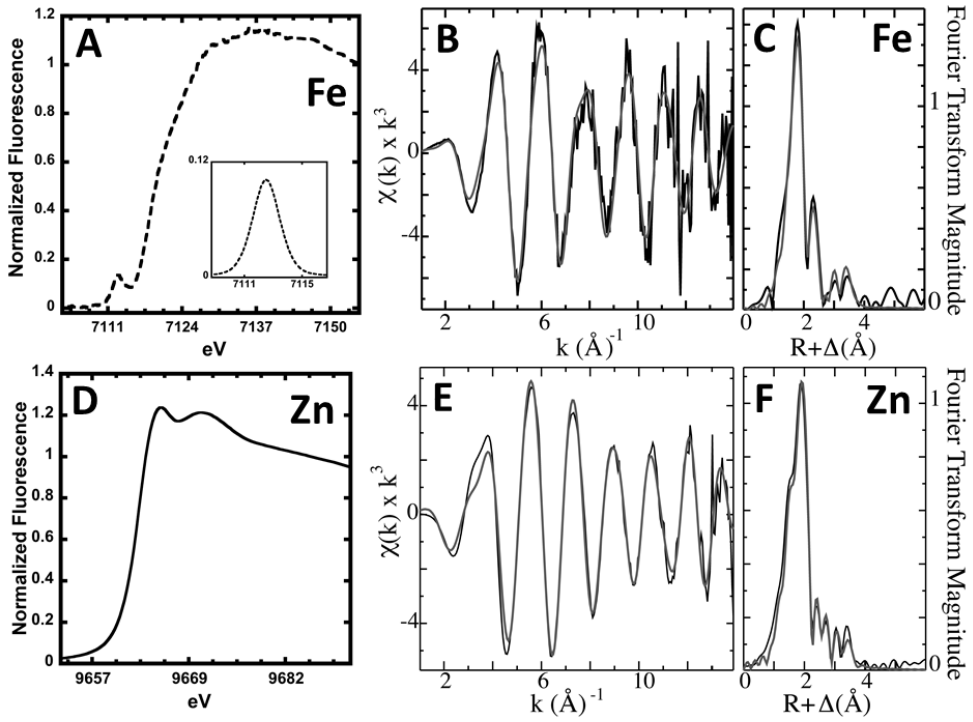

Figure 10. XAS data for the [2Fe-2S] and Zn centers of CPSF30, adapted from reference [54]. Fe XANES data is shown in (A), EXAFS and its fourier transform is shown in (B) and (C) respectively. Zn XANES data is observed in panel (D) while Zn EXAFS and its fourier transform is shown in (E) and (F) respectively. Experimental data are shown in black, and simulations are depicted in grey. Reprinted (adapted) with permission from *Proc. Natl. Acad. Sci. U. S. A.* 2017, 113, 17, 4700-4705.

7.6. EPR

Electron paramagnetic resonance spectroscopy is a technique that detects unpaired electrons and provides information regarding oxidation state and symmetry of the metal site. In this experiment, a sample is placed in a magnet with a precise microwave frequency applied. The magnetic field is then varied, and unpaired electron transitions can be detected. These transitions lead to distinctive spectrum that are used to identify and characterize metal-protein complexes. The peaks observed have associated g values that are indicative of specific metal centers. Zn contains no unpaired electrons and is therefore silent in this technique; however, Fe and Fe-S cluster binding proteins have rich spectroscopy. As an example, proteins containing a [2Fe-2S] cluster in an oxidized $[2Fe\text{-}2S]^{2+}$ state with Fe(III)-Fe(III), the two S=1/2 electrons are coupled, and no signal is observed. However, when reduced to a $[2Fe\text{-}2S]^{1+}$ (Fe(II)-Fe(III)) system, the unpaired electron (S = 1/2) will show a characteristic signal with a g value of ~1.94 [139]. **Figure 11** shows sample EPR data for [2Fe-2S] clusters. **Figure 11A** describes the difference between [2Fe-2S] cluster binding when Grx3 is present as a homodimer utilizing 2 cysteine residues and 2 glutathiones as ligands (top) [158]. When Fra2 is present, a change in g values is observed in the spectra corresponding to the new ligands in the Grx3-Fra2 heterodimer consisting of CC(GSH)H. In **figure 11B** a similar trend is observed in archaeal Rieske-type ferredoxin (ARF) [159]. The wild type protein containing a [2Fe-2S] cluster bound by a CCHH ligand set observed g values of 2.02, 1.90, and 1.81 while the CCCH mutant exhibited g values of 2.00 and 1.92 (**Figure 11B**). These data can be very useful in conjunction with other techniques to characterize

the redox activity and electronic structure of the metal site. For more in depth information on EPR of metalloproteins and Fe-S clusters we refer the reader to these helpful reviews [160-166].

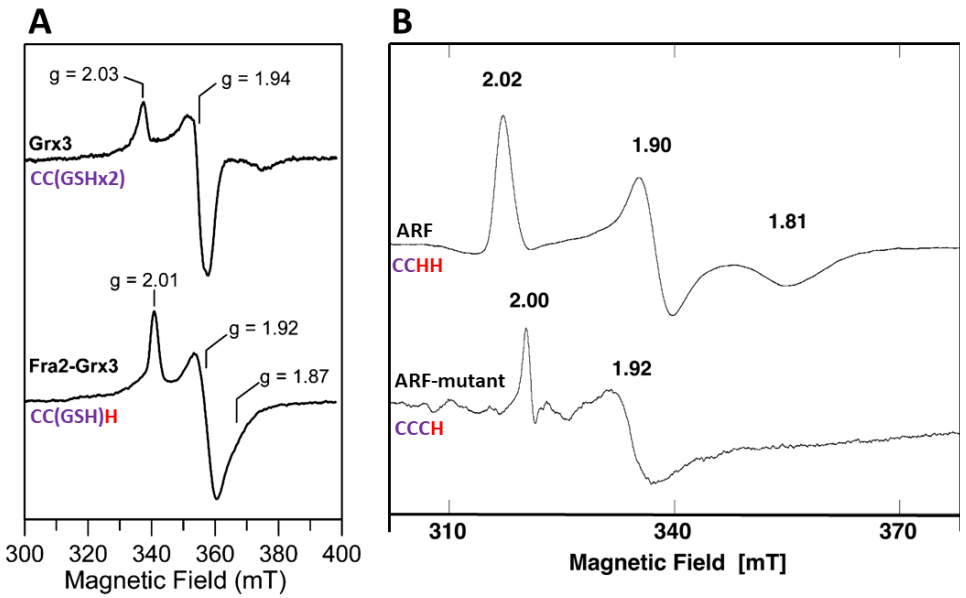

Figure 11. Example EPR data for [2Fe-2S] cluster cofactored proteins adapted from references [158] (A) and [159] (B). The EPR spectra of the Grx3 homodimer (Two cysteine and two glutathione ligands) and Fra2-Grx3 (two cysteine, one glutathione, and one histidine ligands) heterodimers are shown in panel A. Panel B shows the EPR spectra of [2Fe-2S] wild type ARF (top) with a CCHH ligand set and ARF with a mutated CCCH ligand set (bottom). (A) Reprinted (adapted) with permission from *Biochemistry* 2009, 48, 40, 9569-9581. Copyright 2009 American Chemical Society. (B) Reprinted (adapted) with permission from the Creative Commons CC-BY license (*J. Biol. Chem.* 2004, 279, 13, 12519-12528).

7.7. Mössbauer spectroscopy

Mössbauer spectroscopy is specifically utilized for Fe centers in biology and is commonly utilized for Fe-S cluster characterization. Mössbauer requires the enrichment of ^{57}Fe into the metal site which can be accomplished by introducing ^{57}Fe to the media for protein expression or refolding the Fe-S

site using ^{57}Fe metal salts. In the experiment, a gamma photon that is generated from the radioactive decay of ^{57}Co is utilized to monitor the recoilless resonance absorption and emission of gamma irradiation of the Fe site [167]. The absorption and emission spectra of the excited Fe nucleus leads to characteristic signals that report on stoichiometry, redox state, geometry, and electronic properties of the Fe center. Although [2Fe-2S] and [4Fe-4S] clusters both exhibit quadrupole doublets they can be differentiated by their isomer shifts with [2Fe-2S] clusters exhibiting narrower splitting than [4Fe-4S] clusters. In **figure 12A-D**, a Mössbauer spectrum from ^{Nif}IscA protein reported by Johnson and co-workers is presented [168]. The Mössbauer spectrum for ^{Nif}IscA as isolated is shown in panel A where only a $[2Fe\text{-}2S]^{2+}$ spectra is observed. When treated with DTT for 1 (B) and 15 (C) minutes, a conversion of the [2Fe-2S] cluster to [4Fe-4S] cluster is detected. Mössbauer spectroscopy is exceptionally sensitive in differentiating these two cofactor types compared to other spectroscopic methods (e.g., UV-Visible spectroscopy). Panel D shows the conversion of the [4Fe-4S] cluster to a [2Fe-2S] cluster when exposed to oxygen. For more in depth information on Mössbauer spectroscopy of metalloproteins and Fe-S proteins we refer the reader to these helpful reviews [167, 169-171].

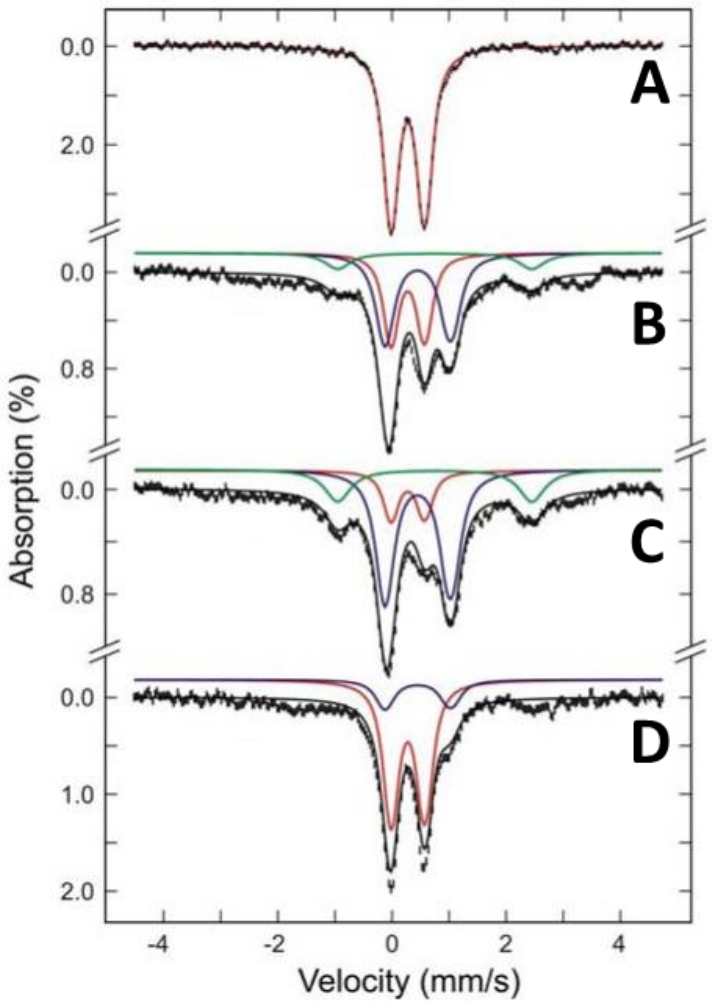

Figure 12. The Mössbauer spectra of ^{Nif}IscA, adapted from reference [168]. The [2Fe-2S] to [4Fe-4S] cluster conversion mediated by DTT addition and its reverse conversion by oxygen addition is observed. Panel A shows the Fe-S cluster of ^{Nif}IscA as isolated in the $[2Fe\text{-}2S]^{2+}$ form. Panels B and C were recorded 1 min and 15 min after DTT addition respectively. Finally, panel D is the observed spectra after sample exposure to air for 5 min after DTT reduction. The green spectra is a simulation of individual Fe(II), while the $[2Fe\text{-}2S]^{2+}$ spectra is simulated in red, and the $[4Fe\text{-}4S]^{2+}$ cluster is simulated in blue. Reprinted (adapted) with permission from reference *Biochemistry* 2012, 51, 41, 8071-8084. Copyright 2012 American Chemical Society.

7.8. Resonance Raman

Resonance Raman (RR) spectroscopy utilizes excitation of vibrational bands that are enhanced by the use of a laser to reduce scattering [30]. RR data can inform on ligand to metal charge transfer bands (LMCT) and π-π^* transitions from ligands (e.g., porphyrin) in metalloproteins. RR has been extensively utilized to characterize Fe-S clusters both in model systems and proteins. A key difference in the RR signal for a [2Fe-2S] (CCCC) versus a [2Fe-2S] (CCCH) system is found in the 250-310 cm^{-1} region. This region in the RR spectra is sensitive to the [2Fe-2S] cluster breathing mode symmetry. [2Fe-2S] clusters with a CCCH ligand set have two bands in this region while [2Fe-2S] clusters with a CCCC ligand set have a singular, broad band. These differences are related to the symmetry of the Fe-S site, and the resonance Raman spectrum can serve as a fingerprint of the ligand set. This method has been employed to delineate the ligand set of the Fe-S clusters in mitoNEET and Grx3-Fra2 complex, shown in Figure 13 (**figure 13A-B**) [158, 172]. For more in depth information on RR spectroscopy of metalloproteins and more specifically Fe-S clusters, we refer the reader to these helpful reviews [173-175].

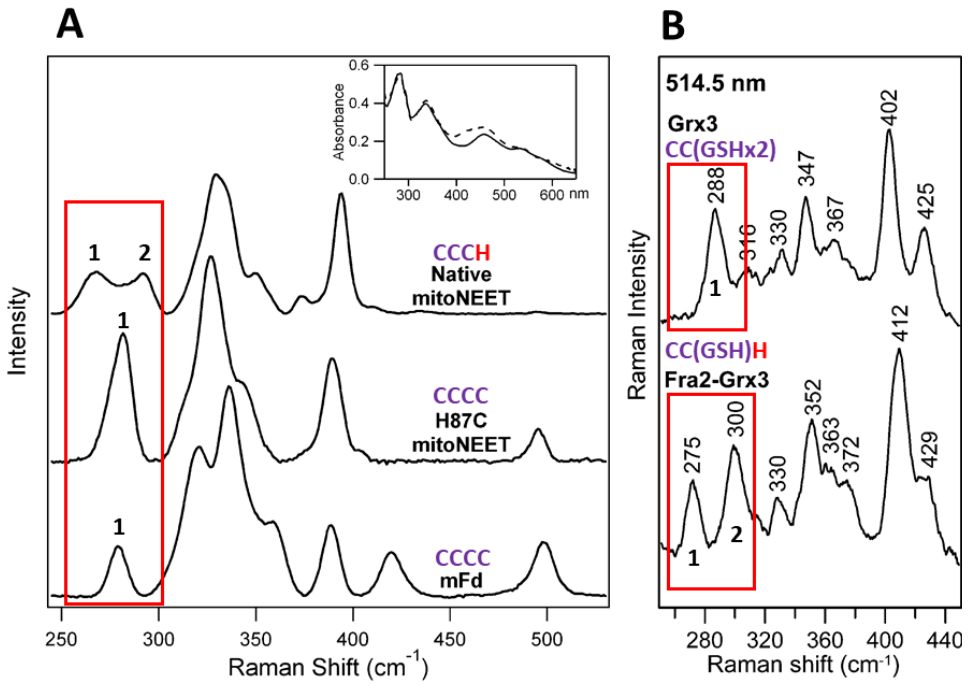

Figure 13. Resonance Raman spectra of mitoNEET, Grx3 homodimer, and Fra2-Grx2 heterodimer adapted from references [158] and [172]. The resonance Raman spectra of wildtype mitoNEET (top A), a 4 cys mutant (middle A), and Mastigocladus *laminosus* ferredoxin (bottom A) are shown. The RR spectra of the Grx3 homodimer and Fra2-Grx3 heterodimer are shown in panel B (top and bottom respectively). The region of the spectrum that is sensitive to CCCH vs CCCC ligation is denoted by a red box. (A) Reprinted (adapted) with permission from *Biochemistry* 2009, 48, 22, 4747-4752. Copyright 2009 American Chemical Society. (B) Reprinted (adapted) with permission from *Biochemistry* 2009, 48, 40, 9569-9581. Copyright 2009 American Chemical Society.

7.9. Circular Dichroism

Circular dichroism (CD) is commonly used to characterize secondary structure (alpha helices and beta sheets) of proteins. Here the data are collected in the ultraviolet regime. CD can also inform on Fe-S cluster charge transfer bands when the spectrum is measured in the far-ultraviolet to visible regime. Here, specific bands are observed, as shown in the spectra of [2Fe-2S] clusters of the Grx3 homodimer and the Fra2-Grx3 heterodimer (**Figure 14**).

This far-UV to visible region of the CD spectra is sensitive to electronic structure differences in the ligation and/or chirality of the protein's [2Fe-2S] cofactor. These data can be challenging to interpret and are typically reported in tandem with other techniques (commonly the ones described in this review) to confirm the identity and geometry of Fe-S cluster sites. For more in depth information on CD of Fe-S clusters we refer the reader to these helpful reviews [122, 176].

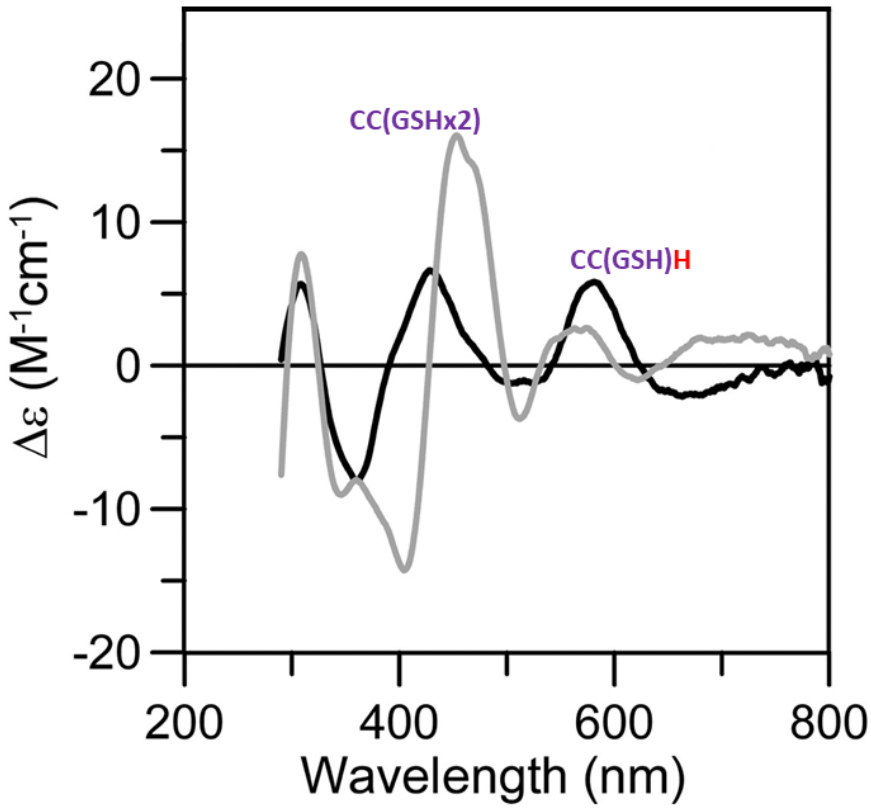

Figure 14. The CD spectra of the Grx3 homodimer bound [2Fe-2S] (grey) and the Grx3-Fra2 complex bound [2Fe-2S] cluster (black). Reprinted (adapted) with permission from *Biochemistry* 2009, 48, 40, 9569-9581. Copyright 2009 American Chemical Society.

7.10. Native Mass spectrometry

Mass spectrometry has traditionally been used in biochemical studies to determine protein molecular weight, with both MALDI and ESI-MS being common approaches. The metal co-factor is not always retained in these measurements, because the sample preparation involves denaturants, or the technique is necessarily harsh causing the metal to dissociate in the gas phase. A milder native electrospray ionization mass spectrometry (ESI-MS) approach in which the protein retains the metal cofactor has been developed in recent years. Native ESI-MS can be used to identify the metal cofactor, determine stoichiometry, and identify intermediates. As an example, in **figure 15** the native ESI-MS of the protein RirA which has a [4Fe-4S] co-factor is shown (**figure 15 black line**) [177]. Multiple Fe-S co-factors are observed in this spectrum likely due to degradation of the [4Fe-4S] cluster during buffer exchange and ionization in the gas phase. When treated with EDTA to limit iron availability, the apo protein becomes the dominant form (**figure 15 red line**) [177]. These data can be utilized in conjunction with other techniques to fully characterize metal cofactors of proteins and we refer the reader to these helpful reviews for more information on these techniques [178-181].

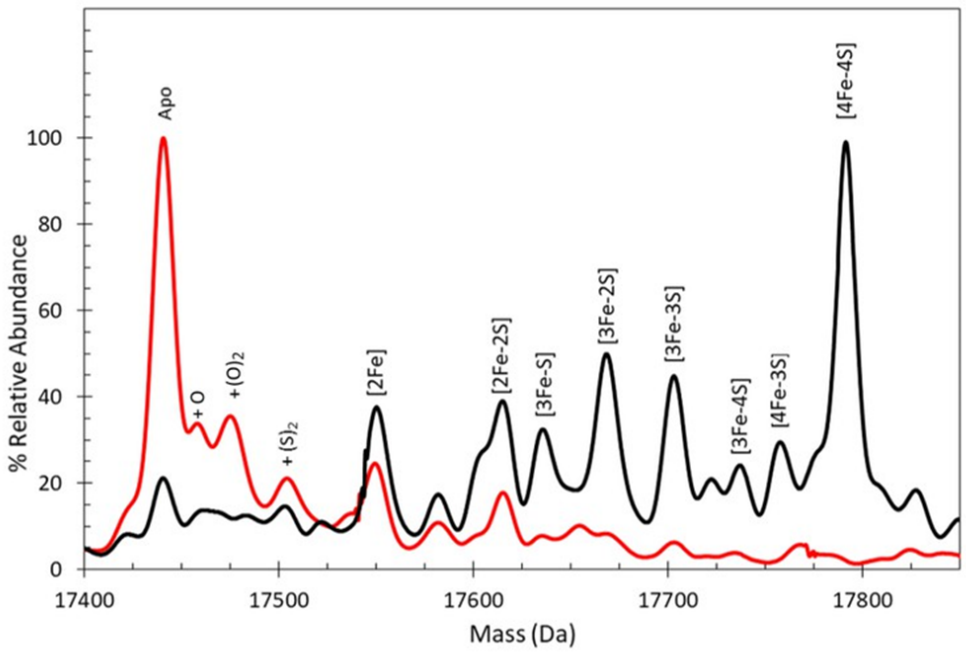

Figure 15. Native ESI-MS data of RirA are shown adapted from reference [177]. The as isolated RirA form is observed in black while the Fe starved (EDTA added) is shown in red. Reprinted (adapted) with permission from the Creative Commons Attribution License (*eLIFE* 2019, 8, e47804). Copyright 2019 Pellicer Martinez et al.

7.11. Mutagenesis

Genetic mutational studies can also be pursued to characterize metalloprotein metal centers. When a protein is annotated as a metal binding protein and/or observed empirically to bind a metal cofactor one might have an educated guess as to which ligands are involved. Mutagenesis can be a helpful technique to verify these predictions. In this approach, specific amino acid ligands can be replaced, and the resultant mutated protein can be characterized to determine the effect on metal binding. A traditional mutagenesis approach involves mutating the side chain of interest to alanine, which has a methyl functional group; however, this mutation can perturb bonding interactions (e.g., hydrogen bonds, electrostatic interactions) that are involved in secondary structure but not necessarily metal binding. Another

approach involves mutating the residue of interest to a similar residue that retains the key non-covalent interactions of the residue, while disrupting metal binding properties. For instance, instead of alanine for cysteine, a mutation of serine for cysteine retains the electrostatic and hydrogen bonding properties of cysteine while abrogating metal binding. As such, a cysteine to serine mutation is a common modification utilized in ligand identification for Fe-S proteins (**Figure 16**). This type of mutagenesis was integral to the study of Fep1 discussed earlier leading to the identification of one of its ZF domains acting as a rescue site for its Fe-S cluster cofactor [56]. Similarly, histidine is often replaced with glutamine as it can mimic the epsilon nitrogen of histidine (**Figure 16**). Both residues contain 3 carbon atoms followed by a nitrogen heteroatom off the peptide backbone. Similarly, asparagine can be utilized to mimic the delta nitrogen of histidine (2 carbons and 1 nitrogen) (**Figure 16**). For more in depth information on mutagenesis studies to investigate metalloproteins we refer the reader to these helpful reviews [182, 183].

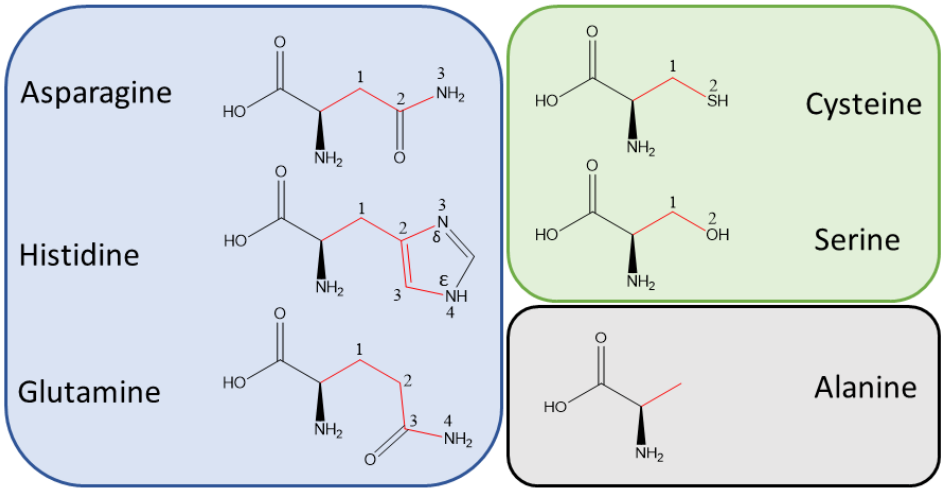

Figure 16. Chemical structures of amino acids to indicate how asparagine and glutamine can be utilized as mutagenesis mimics for histidine and serine can be utilized as a mimic for cysteine instead of alanine.

Table 2: Summary of common techniques to study metalloproteins.

Technique	Uses	Amount of sample needed	Fe-S, Zn, or both	Pros	Cons
UV-Vis	-Protein concentration - Metal centered optical transitions (e.g., charge transfer, d-d)	µM protein	Both (Zn needs Co as a spectroscopic probe)	-Ease of use -Common laboratory instrument -Cost effective -Low amount of training required	-Spectra can be ambiguous -Other techniques needed to confirm
ICP-MS	-Metal Identity -Protein to metal stoichiometry	nM-µM metal	Both	-High accuracy	-Expensive instrument -Specialized training required
XAS	-Oxidation state -Site symmetry -Covalency	High µM to low mM metal	Both	-Identifies metal, ligands and coordination geometry -Solution based	-Need synchrotron access -Highly specialized

	-Electronic structure -Ligands -Coordination number -Ligand distances				training required -Large amount of sample needed
EPR	-Metal Identity -Redox sensitivity -Geometry	High μM to low mM metal	Fe-S	-Highly accurate -Characteristic spectra to compare to	-Highly specialized equipment -Cryo temperatures -Large amount of sample needed -Highly specialized training required
Mössbauer	-Nuclearity -Redox state -Geometry	Low mM metal	Fe-S	- Clear distinction between iron	-Need expensive ^{57}Fe labeling

	-Electronic properties			sulfur cluster types	-Highly specialized instrument -Highly specialized training required -Large amount of sample needed -Highly specialized equipment -Specialized training required -Large amount of sample needed
RR	-Ligand identity	Low mM protein and metal	Both	-Characteristic spectra to compare to	
CD	-Geometry	µM protein/ Fe-S cluster	Fe-S	-Characteristic spectra to compare to	-Moderately Expensive instrument

				-No significant training needed	
Native Mass spec	-Metal identity -Molecular Weight -Metal: ligand Stoichiometry -Detects reaction intermediates	Low μM	Both	-Provides information on native protein	-Expensive instrument -Highly specialized training required
Mutagenesis	-Ligand identification	Varies	Both	-Cost effective -Not much additional training required in protein biochemistry labs	-Time and optimization requirements

7.12 Synthetic Model Complexes of Fe-S Clusters

While the synthetic model approach is not discussed explicitly in this review, it would be remiss not to point out the pioneering work of Dick Holm in this area. Starting in the early 1970s, it was recognized that Fe-S centers could be prepared synthetically using carefully designed ligands. These findings led to a proliferation of publications describing small molecule

mimetics of Fe-S centers, much of which was led by Holm [184, 185]. This work provided an understanding of the structure and reactivity of numerous types of Fe-S clusters from which fundamental principles concerning Fe-S cluster reactivity were obtained. Working with small molecule mimetics helped circumvent the fragility of protein bound clusters in aqueous buffers allowing research to be conducted in organic solvents [186]. Streamlining the metal site to the primary coordination sphere allowed for the complex to be studied at higher concentrations for spectroscopic measurements and simplified the reagents to study catalytic and redox reaction mechanisms. These synthetic mimetics were extremely helpful in identifying reaction intermediates, determining how Fe-S clusters can be self-assembled, and controlling nuclearity [184, 186]. Additionally, as proteins with Fe-S cluster co-factors were isolated, comparisons could be made to data obtained for Fe-S cluster model complexes providing deeper insight into these proteins' properties and reactivity [184, 186]. Particularly relevant to this review are recent synthetic models of mitoNEET reported by Mayer and Meyer [73]. The reported complex was the first example of a model complex of a 2Fe-2S cluster with a 3Cys/1His ligand set, and it was demonstrated that the cluster could undergo proton coupled electron transfer with TEMPO, suggesting a possible biological function [73].

8. Additional considerations

In this review, we have focused on the in vitro characterization of several annotated ZFs that were found to be active with an iron-sulfur cluster co-factor. The characterization of singular proteins teaches us which metals can serve as co-factors on the molecular level. These data provide us a piece of the puzzle of metal:protein pairing, which can be complemented by studies of proteins directly in cells. In the cell, the metal:protein pairing paradigm is more complex as metal availability is regulated by additional factors (other proteins, signaling pathways, etc.). As such, we are just beginning to unravel the complexities of metal homeostasis in cells. Work by a number of laboratories has shown that metal homeostasis is impacted by metal availability and an emerging concept is that of metallostasis, whereby a suite of proteins (importers, exporters, sensors, and storage proteins) control levels of available metals in specific cellular locations and compartments. This allows for metal levels to be finely tuned to ensure that mis-metallation does not occur [2, 3, 9, 187-189]. One key class of proteins that play a role in metal homeostasis/metallostasis are metallochaperones. Metallochaperones function to bind and transport metals to particular protein targets. These types of proteins were first identified in copper, (e.g., ATX1, CCS, COPZ), [9, 11] . For Fe-S clusters, the metal:protein paradigm includes proteins involved in biosynthesis, regulation, and chaperoning Fe-S clusters. In eukaryotes, these proteins are found in the mitochondria, cytoplasm, and nucleus of eukaryotic cells where they are part of the SUF (sulfur mobilization), ISC (iron-sulfur cluster assembly), and CIA (cytosolic iron-sulfur protein assembly) pathways. [14, 190, 191]. For zinc, it has been challenging to identify a

metallochaperone; however there is new work that has identified a bacterial chaperone (e.g., ZigA) [192]. In eukaryotes, the zinc chaperone remains elusive, but its presence is hinted at in a compelling study of the protein ALAD, which is an Fe-S cluster protein involved in heme biosynthesis. This protein can be assembled with a 4Fe-4S cluster or isolated with a zinc co-factor in vitro, with the Fe-S co-factored protein showing greater enzymatic activity. In cells, the protein can only be loaded with the Fe-S cofactor, addition of zinc results in increased metallothionein (a zinc binding protein) but has no effect on ALAD activity, suggesting that a zinc chaperone to deliver zinc to ALAD is not present [58]. Of note is the presence of metallothionein, which is known to be regulated by zinc. When cellular zinc concentrations are high, thionein (the apo-form of metallothionein) is expressed and sequesters zinc. When cellular zinc proteins require zinc, zinc dissociates from metallothionein and thionein is regenerated. This paradigm is influenced by many factors including other metal ions, cellular localization, redox chemistry, and pH, illustrating the complexity of metal regulation in cells [193]. A more detailed discussion of the myriad of dynamic roles for metallothionein can be found in a recent *Chem. Rev.* article [193].

When metal homeostasis is disrupted, proteins are susceptible to binding other metals. In isolation, metal binding to proteins is driven by thermodynamics, and follows the Irving-Williams series (Mn < Fe < Co < Ni < Cu, Zn) [3, 187]. The cell overcomes this thermodynamic preference by limiting 'free metals' – (free metal concentrations follow Cu < Zn < Ni < Co < Fe < Mn < Ca < Mg) and compartmentalizing certain metals [3]. Notably, the total metal concentrations in the cell follow Co, Ni < Mn < Cu < Fe, Zn trends

[3]. Although Fe and Zn are the most abundant metals, they are also the most tightly regulated [3]. Compounding these observations is the finding that metal concentrations vary widely between cell types and within species (e.g., liver versus heart cells) [3].

The examples given in this review speak to the challenge of identifying a protein's 'correct' metal co-factor both in vitro and in cells. It is known that a number of Fe-S cluster proteins have been mistakenly purified from *E. coli* with Zn in their metal sites [55, 58, 134]. Fe-S cluster sites are more easily degraded and lost in protein centers because of their susceptibility to oxidation, whereas Zn binds tightly and this thermodynamic preference for zinc when isolating proteins may explain why these Fe-S proteins are isolated with a Zn co-factor. Strategies to circumvent this issue, and verify the correct co-factor include varying the concentrations of zinc and iron present during protein expression, upregulating the Fe-S cluster machinery, or expressing the protein in its native host. Additionally, when the correct metal cofactor is ambiguous, functional assays that test the activity of the protein can inform on the functional co-factor. It can be challenging to identify the "correct" metal co-factor of a newly isolated metalloprotein; however, for Zn and Fe-S co-factored proteins, we have a growing arsenal of tools that aid in this identification (Table 2).

9. Conclusions

The advancement of computer processing and whole genome sequencing has led to significant advances in the annotation of genomes. From this wealth of information, the number of predicted proteins and their

associated functions has increased similarly. However, recent examples of incorrect annotations through these *in silico* methods underscores the need for empirical validation of these proteins' functions and cofactors. In this review, we have illustrated this need for empirical validation with the examples of mitoNEET, CPSF30, nsp12, and Fep1. These proteins were all annotated as zinc binding proteins, but empirically determined to bind Fe-S clusters instead. This mis-annotation is not limited to Zn and Fe-S clusters. As an example, ATE1 was annotated as a heme binding protein, but was discovered to harbor an Fe-S cluster when studied empirically [194]. An awareness of the flexibility of metal sites is important as we study new metalloproteins to understand their fundamental biological roles.

10. Abbreviations

Zinc finger proteins, ZFs; Cleavage and Polyadenylation Specificity Factor 30, CPSF30, CPSF4; Nonstructural protein 12, nsp12; Iron-sensing transcriptional repressor, Fep1; thiazolidinediones, TZD; Iron-sulfur cluster, Fe-S; Electron Paramagnetic Resonance, EPR; Polyadenylation signal, PAS; Tristetraprolin, TTP; Maltose binding protein, MBP; X-ray absorption spectroscopy, XAS; inductively coupled plasma mass spectrometry, ICP-MS; Fluorescence anisotropy, FA; Severe acute respiratory syndrome coronavirus 2, SARS-CoV-2; RNA-dependent RNA polymerase, RdRp; Cryogenic Electron Microscopy, Cryo-EM; Heat shock protein cognate 20, HSC-20; Coimmunoprecipitation, Co-IP; Iron-sulfur cluster assembly scaffold protein, ISCU; 4-hydroxy-2,2,6,6-tetramethylpiperidin-1-oxyl, 4-Hydroxy-TEMPO, TEMPOL; Sterol regulatory element-binding protein 1, SRE-1; Inductively

coupled plasma atomic emission spectroscopy, ICP-AES; UV-visible spectroscopy, UV-vis; Resonance Raman, RR; Circular dichroism, CD; Electrospray ionization mass spectrometry, ESI-MS; Matrix assisted laser desorption ionization mass spectrometry, MALDI-MS;

Funding:

SLJM is grateful for funding from the NSF (CHE-1708732 and CHE-2106417), JDP is grateful for funding from the NIH (T32, GM066706) and AFPE.

Declaration of competing interests.

None.

References

[1] K.J. Waldron, N.J. Robinson, How do bacterial cells ensure that metalloproteins get the correct metal?, Nat. Rev. Microbiol., 7, 1, (2009), 25-35, https://doi.org/10.1038/nrmicro2057

[2] K.J. Waldron, J.C. Rutherford, D. Ford, N.J. Robinson, Metalloproteins and metal sensing, Nature, 460, 7257, (2009), 823-830, https://doi.org/10.1038/nature08300

[3] W. Maret, Metalloproteomics, metalloproteomes, and the annotation of metalloproteins, Metallomics, 2, 2, (2010), 117-125, https://doi.org/10.1039/b915804a

[4] C.L. Dupont, S. Yang, B. Palenik, P.E. Bourne, Modern proteomes contain putative imprints of ancient shifts in trace metal geochemistry, Proc. Natl. Acad. Sci. U. S. A., 103, 47, (2006), 17822-17827, https://doi.org/10.1073/pnas.0605798103

[5] C. Andreini, I. Bertini, A. Rosato, A hint to search for metalloproteins in gene banks, Bioinformatics, 20, 9, (2004), 1373-1380, https://doi.org/10.1093/bioinformatics/bth095

[6] I. Bertini, G. Cavallaro, Metals in the "omics" world: copper homeostasis and cytochrome c oxidase assembly in a new light, J. Biol. Inorg. Chem., 13, 1, (2008), 3-14, https://doi.org/10.1007/s00775-007-0316-9

[7] W. Maret, Zinc and the zinc proteome, Met. Ions Life Sci., 12, (2013), 479-501, https://doi.org/10.1007/978-94-007-5561-1_14

[8] F.E. Duncan, E.L. Que, N. Zhang, E.C. Feinberg, T.V. O'Halloran, T.K. Woodruff, The zinc spark is an inorganic signature of human egg activation, Sci. Rep., 6, 1, (2016), 24737, https://doi.org/10.1038/srep24737

[9] T.V. O'Halloran, V.C. Culotta, Metallochaperones, an Intracellular Shuttle Service for Metal Ions *, J. Biol. Chem., 275, 33, (2000), 25057-25060, https://doi.org/10.1074/jbc.R000006200

[10] M. Gupta, C.E. Outten, Iron–sulfur cluster signaling: The common thread in fungal iron regulation, Curr. Opin. Chem. Biol., 55, (2020), 189-201, https://doi.org/https://doi.org/10.1016/j.cbpa.2020.02.008

[11] A.C. Rosenzweig, T.V. O'Halloran, Structure and chemistry of the copper chaperone proteins, Curr. Opin. Chem. Biol., 4, 2, (2000), 140-147, https://doi.org/10.1016/s1367-5931(99)00066-6

[12] E.L. Que, R. Bleher, F.E. Duncan, B.Y. Kong, S.C. Gleber, S. Vogt, S. Chen, S.A. Garwin, A.R. Bayer, V.P. Dravid, T.K. Woodruff, T.V. O'Halloran, Quantitative mapping of zinc fluxes in the mammalian egg reveals the origin of fertilization-induced zinc sparks, Nat. Chem., 7, 2, (2015), 130-139, https://doi.org/10.1038/nchem.2133

[13] W.W. Fischer, J. Hemp, J.S. Valentine, How did life survive Earth's great oxygenation?, Curr. Opin. Chem. Biol., 31, (2016), 166-178, https://doi.org/https://doi.org/10.1016/j.cbpa.2016.03.013

[14] J.J. Braymer, S.A. Freibert, M. Rakwalska-Bange, R. Lill, Mechanistic concepts of iron-sulfur protein biogenesis in Biology, Biochim. Biophys. Acta, Mol. Cell Res., 1868, 1, (2021), 118863, https://doi.org/https://doi.org/10.1016/j.bbamcr.2020.118863

[15] R.J.P. Williams, Iron in evolution, FEBS Lett., 586, 5, (2012), 479-484, https://doi.org/https://doi.org/10.1016/j.febslet.2011.05.068

[16] R.P. Hong Enriquez, T.N. Do, Bioavailability of metal ions and evolutionary adaptation, Life, 2, 4, (2012), 274-285, https://doi.org/10.3390/life2040274
[17] M.W.C. J. D. Hem, in: U.S.D.O.T. INTERIOR (Ed.), United States Government Printing Office, The U.S. Geological Survey Library, 1962.
[18] H. Eom, W.J. Song, Emergence of metal selectivity and promiscuity in metalloenzymes, JBIC, J. Biol. Inorg. Chem., 24, 4, (2019), 517-531, https://doi.org/10.1007/s00775-019-01667-0
[19] R.J. Williams, Zinc in evolution, J. Inorg. Biochem., 111, (2012), 104-109, https://doi.org/10.1016/j.jinorgbio.2012.01.004
[20] G.T. Antelo, A.J. Vila, D.P. Giedroc, D.A. Capdevila, Molecular Evolution of Transition Metal Bioavailability at the Host-Pathogen Interface, Trends Microbiol., 29, 5, (2021), 441-457, https://doi.org/10.1016/j.tim.2020.08.001
[21] C. Andreini, L. Banci, I. Bertini, A. Rosato, Zinc through the Three Domains of Life, J. Proteome Res., 5, 11, (2006), 3173-3178, https://doi.org/10.1021/pr0603699
[22] R.O. Emerson, J.H. Thomas, Adaptive Evolution in Zinc Finger Transcription Factors, PLoS Genet., 5, 1, (2009), e1000325, https://doi.org/10.1371/journal.pgen.1000325
[23] N.D. Clarke, J.M. Berg, Zinc fingers in Caenorhabditis elegans: finding families and probing pathways, Science, 282, 5396, (1998), 2018-2022, https://doi.org/10.1126/science.282.5396.2018
[24] D.R. Engelke, S.Y. Ng, B.S. Shastry, R.G. Roeder, Specific interaction of a purified transcription factor with an internal control region of 5S RNA genes, Cell, 19, 3, (1980), 717-728, https://doi.org/10.1016/s0092-8674(80)80048-1
[25] D.R. Smith, I.J. Jackson, D.D. Brown, Domains of the positive transcription factor specific for the Xenopus 5S RNA gene, Cell, 37, 2, (1984), 645-652, https://doi.org/10.1016/0092-8674(84)90396-9
[26] J.S. Hanas, D.J. Hazuda, D.F. Bogenhagen, F.Y. Wu, C.W. Wu, Xenopus transcription factor A requires zinc for binding to the 5 S RNA gene, J. Biol. Chem., 258, 23, (1983), 14120-14125,
[27] R.S. Brown, C. Sander, P. Argos, The primary structure of transcription factor TFIIIA has 12 consecutive repeats, FEBS Lett., 186, 2, (1985), 271-274, https://doi.org/10.1016/0014-5793(85)80723-7
[28] J. Miller, A.D. McLachlan, A. Klug, Repetitive zinc-binding domains in the protein transcription factor IIIA from Xenopus oocytes, EMBO J., 4, 6, (1985), 1609-1614,
[29] J.M. Berg, Zinc Finger Domains: Hypotheses and Current Knowledge, Annu. Rev. Biophys. Biophys. Chem., 19, 1, (1990), 405-421, https://doi.org/10.1146/annurev.bb.19.060190.002201
[30] S.J. Lippard, J.M. Berg, Principles of Bioinorganic Chemistry (1994)
[31] R.G. Pearson, Hard and Soft Acids and Bases, J. Am. Chem. Soc., 85, 22, (1963), 3533-3539, https://doi.org/10.1021/ja00905a001
[32] R.G. Pearson, Hard and soft acids and bases, HSAB, part 1: Fundamental principles, J. Chem. Educ., 45, 9, (1968), 581, https://doi.org/10.1021/ed045p581
[33] R.G. Pearson, Hard and soft acids and bases, HSAB, part II: Underlying theories, J. Chem. Educ., 45, 10, (1968), 643, https://doi.org/10.1021/ed045p643
[34] J.M. Berg, Proposed structure for the zinc-binding domains from transcription factor IIIA and related proteins, Proc. Natl. Acad. Sci. U. S. A., 85, 1, (1988), 99-102, https://doi.org/10.1073/pnas.85.1.99
[35] R.S. Brown, P. Argos, Fingers and helices, Nature, 324, 6094, (1986), 215, https://doi.org/10.1038/324215a0

[36] N.P. Pavletich, C.O. Pabo, Zinc finger-DNA recognition: crystal structure of a Zif268-DNA complex at 2.1 A, Science, 252, 5007, (1991), 809-817, https://doi.org/10.1126/science.2028256
[37] N.P. Pavletich, C.O. Pabo, Crystal structure of a five-finger GLI-DNA complex: new perspectives on zinc fingers, Science, 261, 5129, (1993), 1701-1707, https://doi.org/10.1126/science.8378770
[38] D. Wang, J.R. Horton, Y. Zheng, R.M. Blumenthal, X. Zhang, X. Cheng, Role for first zinc finger of WT1 in DNA sequence specificity: Denys-Drash syndrome-associated WT1 mutant in ZF1 enhances affinity for a subset of WT1 binding sites, Nucleic Acids Res., 46, 8, (2018), 3864-3877, https://doi.org/10.1093/nar/gkx1274
[39] B.L. Vallee, D.S. Auld, Zinc coordination, function, and structure of zinc enzymes and other proteins, Biochemistry, 29, 24, (1990), 5647-5659, https://doi.org/10.1021/bi00476a001
[40] K. Kluska, J. Adamczyk, A. Krężel, Metal binding properties, stability and reactivity of zinc fingers, Coord. Chem. Rev., 367, (2018), 18-64, https://doi.org/10.1016/j.ccr.2018.04.009
[41] S.J. Lee, S.L. Michel, Structural metal sites in nonclassical zinc finger proteins involved in transcriptional and translational regulation, Acc. Chem. Res., 47, 8, (2014), 2643-2650,
[42] M.A. Searles, D. Lu, A. Klug, The role of the central zinc fingers of transcription factor IIIA in binding to 5 S RNA, J. Mol. Biol., 301, 1, (2000), 47-60, https://doi.org/10.1006/jmbi.2000.3946
[43] A. Klug, The Discovery of Zinc Fingers and Their Applications in Gene Regulation and Genome Manipulation, Annu. Rev. Biochem., 79, 1, (2010), 213-231, https://doi.org/10.1146/annurev-biochem-010909-095056
[44] L. Decaria, I. Bertini, R.J. Williams, Zinc proteomes, phylogenetics and evolution, Metallomics, 2, 10, (2010), 706-709, https://doi.org/10.1039/c0mt00024h
[45] J.L. Michalek, A.N. Besold, S.L. Michel, Cysteine and histidine shuffling: mixing and matching cysteine and histidine residues in zinc finger proteins to afford different folds and function, Dalton Trans., 40, 47, (2011), 12619-12632, https://doi.org/10.1039/c1dt11071c
[46] J.H. Laity, B.M. Lee, P.E. Wright, Zinc finger proteins: new insights into structural and functional diversity, Curr. Opin. Struct. Biol., 11, 1, (2001), 39-46, https://doi.org/https://doi.org/10.1016/S0959-440X(00)00167-6
[47] W. Maret, New perspectives of zinc coordination environments in proteins, J. Inorg. Biochem., 111, (2012), 110-116, https://doi.org/https://doi.org/10.1016/j.jinorgbio.2011.11.018
[48] S.S. Krishna, I. Majumdar, N.V. Grishin, Structural classification of zinc fingers, Nucleic Acids Res., 31, 2, (2003), 532-550, https://doi.org/10.1093/nar/gkg161
[49] B.A. Krizek, D.L. Merkle, J.M. Berg, Ligand variation and metal ion binding specificity in zinc finger peptides, Inorg. Chem., 32, 6, (1993), 937-940, https://doi.org/10.1021/ic00058a030
[50] K. Ok, M.R. Filipovic, S.L.J. Michel, Targeting Zinc Finger Proteins with Exogenous Metals and Molecules: Lessons Learned from Tristetraprolin, a CCCH type Zinc Finger, Eur. J. Inorg. Chem., (2021), https://doi.org/https://doi.org/10.1002/ejic.202100402
[51] C. Andreini, L. Banci, I. Bertini, A. Rosato, Counting the zinc-proteins encoded in the human genome, J. Proteome Res., 5, 1, (2006), 196-201, https://doi.org/10.1021/pr050361j

[52] A. Passerini, C. Andreini, S. Menchetti, A. Rosato, P. Frasconi, Predicting zinc binding at the proteome level, BMC Bioinf., 8, (2007), 39-39, https://doi.org/10.1186/1471-2105-8-39
[53] I. Bertini, L. Decaria, A. Rosato, The annotation of full zinc proteomes, J. Biol. Inorg. Chem., 15, 7, (2010), 1071-1078, https://doi.org/10.1007/s00775-010-0666-6
[54] G.D. Shimberg, J.L. Michalek, A.A. Oluyadi, A.V. Rodrigues, B.E. Zucconi, H.M. Neu, S. Ghosh, K. Sureschandra, G.M. Wilson, T.L. Stemmler, S.L.J. Michel, Cleavage and polyadenylation specificity factor 30: An RNA-binding zinc-finger protein with an unexpected 2Fe–2S cluster, Proc. Natl. Acad. Sci. U. S. A., 113, 17, (2016), 4700-4705, https://doi.org/10.1073/pnas.1517620113
[55] N. Maio, B.A.P. Lafont, D. Sil, Y. Li, J.M. Bollinger, Jr., C. Krebs, T.C. Pierson, W.M. Linehan, T.A. Rouault, Fe-S cofactors in the SARS-CoV-2 RNA-dependent RNA polymerase are potential antiviral targets, Science, 373, 6551, (2021), 236-241, https://doi.org/10.1126/science.abi5224
[56] A. Cutone, B.D. Howes, A.E. Miele, R. Miele, A. Giorgi, A. Battistoni, G. Smulevich, G. Musci, M.C. di Patti, Pichia pastoris Fep1 is a [2Fe-2S] protein with a Zn finger that displays an unusual oxygen-dependent role in cluster binding, Sci. Rep., 6, (2016), 31872, https://doi.org/10.1038/srep31872
[57] S.E. Wiley, M.L. Paddock, E.C. Abresch, L. Gross, P. van der Geer, R. Nechushtai, A.N. Murphy, P.A. Jennings, J.E. Dixon, The Outer Mitochondrial Membrane Protein mitoNEET Contains a Novel Redox-active 2Fe-2S Cluster, J. Biol. Chem., 282, 33, (2007), 23745-23749, https://doi.org/10.1074/jbc.C700107200
[58] G. Liu, D. Sil, N. Maio, W.-H. Tong, J.M. Bollinger, C. Krebs, T.A. Rouault, Heme biosynthesis depends on previously unrecognized acquisition of iron-sulfur cofactors in human amino-levulinic acid dehydratase, Nat. Commun., 11, 1, (2020), 6310, https://doi.org/10.1038/s41467-020-20145-9
[59] N. Maio, A. Singh, H. Uhrigshardt, N. Saxena, W.H. Tong, T.A. Rouault, Cochaperone binding to LYR motifs confers specificity of iron sulfur cluster delivery, Cell Metab., 19, 3, (2014), 445-457, https://doi.org/10.1016/j.cmet.2014.01.015
[60] N. Maio, T.A. Rouault, Iron-sulfur cluster biogenesis in mammalian cells: New insights into the molecular mechanisms of cluster delivery, Biochim. Biophys. Acta, 1853, 6, (2015), 1493-1512, https://doi.org/10.1016/j.bbamcr.2014.09.009
[61] K.S. Kim, N. Maio, A. Singh, T.A. Rouault, Cytosolic HSC20 integrates de novo iron-sulfur cluster biogenesis with the CIAO1-mediated transfer to recipients, Hum. Mol. Genet., 27, 5, (2018), 837-852, https://doi.org/10.1093/hmg/ddy004
[62] L. Belmonte, S.S. Mansy, Patterns of Ligands Coordinated to Metallocofactors Extracted from the Protein Data Bank, J. Chem. Inf. Model., 57, 12, (2017), 3162-3171, https://doi.org/10.1021/acs.jcim.7b00468
[63] S.A. Freibert, B.D. Weiler, E. Bill, A.J. Pierik, U. Mühlenhoff, R. Lill, Biochemical Reconstitution and Spectroscopic Analysis of Iron-Sulfur Proteins, Methods Enzymol., 599, (2018), 197-226, https://doi.org/10.1016/bs.mie.2017.11.034
[64] H. Eklund, B. Nordstrom, E. Zeppezauer, G. Soderlund, I. Ohlsson, T. Boiwe, B.O. Soderberg, O. Tapia, C.I. Branden, A. Akeson, Three-dimensional structure of horse liver alcohol dehydrogenase at 2-4 A resolution, J Mol Biol, 102, 1, (1976), 27-59, https://doi.org/10.1016/0022-2836(76)90072-3
[65] X. Wang, H.S. Lee, F.J. Sugar, F.E. Jenney, Jr., M.W. Adams, J.H. Prestegard, PF0610, a novel winged helix-turn-helix variant possessing a rubredoxin-like Zn ribbon motif from the hyperthermophilic archaeon, Pyrococcus furiosus, Biochemistry, 46, 3, (2007), 752-761, https://doi.org/10.1021/bi061870h

[66] J.A. Lowry, W.R. Atchley, Molecular evolution of the GATA family of transcription factors: conservation within the DNA-binding domain, J. Mol. Evol., 50, 2, (2000), 103-115, https://doi.org/10.1007/s002399910012
[67] S.M. Ireland, A.C.R. Martin, ZincBind—the database of zinc binding sites, Database, 2019, (2019), https://doi.org/10.1093/database/baz006
[68] J.R. Colca, W.G. McDonald, D.J. Waldon, J.W. Leone, J.M. Lull, C.A. Bannow, E.T. Lund, W.R. Mathews, Identification of a novel mitochondrial protein ("mitoNEET") cross-linked specifically by a thiazolidinedione photoprobe, Am. J. Physiol. Endocrinol. Metab., 286, 2, (2004), E252-E260, https://doi.org/10.1152/ajpendo.00424.2003
[69] S.E. Wiley, A.N. Murphy, S.A. Ross, P. van der Geer, J.E. Dixon, MitoNEET is an iron-containing outer mitochondrial membrane protein that regulates oxidative capacity, Proc. Natl. Acad. Sci. U. S. A., 104, 13, (2007), 5318-5323, https://doi.org/10.1073/pnas.0701078104
[70] C.H. Lipper, O. Karmi, Y.S. Sohn, M. Darash-Yahana, H. Lammert, L. Song, A. Liu, R. Mittler, R. Nechushtai, J.N. Onuchic, P.A. Jennings, Structure of the human monomeric NEET protein MiNT and its role in regulating iron and reactive oxygen species in cancer cells, Proc. Natl. Acad. Sci. U. S. A., 115, 2, (2018), 272-277, https://doi.org/10.1073/pnas.1715842115
[71] D.W. Bak, S.J. Elliott, Conserved Hydrogen Bonding Networks of MitoNEET Tune FeS Cluster Binding and Structural Stability, Biochemistry, 52, 27, (2013), 4687-4696, https://doi.org/10.1021/bi400540m
[72] E.L. Baxter, P.A. Jennings, J.N. Onuchic, Strand swapping regulates the iron-sulfur cluster in the diabetes drug target mitoNEET, Proc. Natl. Acad. Sci. U. S. A., 109, 6, (2012), 1955-1960, https://doi.org/10.1073/pnas.1116369109
[73] M. Bergner, S. Dechert, S. Demeshko, C. Kupper, J.M. Mayer, F. Meyer, Model of the MitoNEET [2Fe−2S] Cluster Shows Proton Coupled Electron Transfer, J. Am. Chem. Soc., 139, 2, (2017), 701-707, https://doi.org/10.1021/jacs.6b09180
[74] M.M. Dicus, A. Conlan, R. Nechushtai, P.A. Jennings, M.L. Paddock, R.D. Britt, S. Stoll, Binding of histidine in the (Cys)3(His)1-coordinated [2Fe-2S] cluster of human mitoNEET, J. Am. Chem. Soc., 132, 6, (2010), 2037-2049, https://doi.org/10.1021/ja909359g
[75] L.B. Gee, V. Pelmenschikov, C. Mons, N. Mishra, H. Wang, Y. Yoda, K. Tamasaku, M.-P. Golinelli-Cohen, S.P. Cramer, NRVS and DFT of MitoNEET: Understanding the Special Vibrational Structure of a [2Fe-2S] Cluster with (Cys)3(His)1 Ligation, Biochemistry, (2021), https://doi.org/10.1021/acs.biochem.1c00252
[76] T. Iwasaki, R.I. Samoilova, A. Kounosu, D. Ohmori, S.A. Dikanov, Continuous-wave and pulsed EPR characterization of the [2Fe-2S](Cys)3(His)1 cluster in rat MitoNEET, J. Am. Chem. Soc., 131, 38, (2009), 13659-13667, https://doi.org/10.1021/ja903228w
[77] C.H. Lipper, M.L. Paddock, J.N. Onuchic, R. Mittler, R. Nechushtai, P.A. Jennings, Cancer-Related NEET Proteins Transfer 2Fe-2S Clusters to Anamorsin, a Protein Required for Cytosolic Iron-Sulfur Cluster Biogenesis, PLoS One, 10, 10, (2015), e0139699, https://doi.org/10.1371/journal.pone.0139699
[78] Y. Wang, A.P. Landry, H. Ding, The mitochondrial outer membrane protein mitoNEET is a redox enzyme catalyzing electron transfer from FMNH2 to oxygen or ubiquinone, J. Biol. Chem., 292, 24, (2017), 10061-10067, https://doi.org/10.1074/jbc.M117.789800
[79] R. Mittler, M. Darash-Yahana, Y.S. Sohn, F. Bai, L. Song, I.Z. Cabantchik, P.A. Jennings, J.N. Onuchic, R. Nechushtai, NEET Proteins: A New Link Between Iron

Metabolism, Reactive Oxygen Species, and Cancer, Antioxid. Redox Signaling, 30, 8, (2019), 1083-1095, https://doi.org/10.1089/ars.2018.7502
[80] O. Karmi, H.B. Marjault, L. Pesce, P. Carloni, J.N. Onuchic, P.A. Jennings, R. Mittler, R. Nechushtai, The unique fold and lability of the [2Fe-2S] clusters of NEET proteins mediate their key functions in health and disease, J. Biol. Inorg. Chem., 23, 4, (2018), 599-612, https://doi.org/10.1007/s00775-018-1538-8
[81] L. Pesce, V. Calandrini, H.B. Marjault, C.H. Lipper, G. Rossetti, R. Mittler, P.A. Jennings, A. Bauer, R. Nechushtai, P. Carloni, Molecular Dynamics Simulations of the [2Fe-2S] Cluster-Binding Domain of NEET Proteins Reveal Key Molecular Determinants That Induce Their Cluster Transfer/Release, J. Phys. Chem. B, 121, 47, (2017), 10648-10656, https://doi.org/10.1021/acs.jpcb.7b10584
[82] K. Zuo, H.B. Marjault, K.L. Bren, G. Rossetti, R. Nechushtai, P. Carloni, The two redox states of the human NEET proteins' [2Fe-2S] clusters, J. Biol. Inorg. Chem., (2021), https://doi.org/10.1007/s00775-021-01890-8
[83] S.L. Chan, I. Huppertz, C. Yao, L. Weng, J.J. Moresco, J.R. Yates, 3rd, J. Ule, J.L. Manley, Y. Shi, CPSF30 and Wdr33 directly bind to AAUAAA in mammalian mRNA 3' processing, Genes Dev., 28, 21, (2014), 2370-2380, https://doi.org/10.1101/gad.250993.114
[84] M. Clerici, M. Faini, R. Aebersold, M. Jinek, Structural insights into the assembly and polyA signal recognition mechanism of the human CPSF complex, eLife, 6, (2017), e33111, https://doi.org/10.7554/eLife.33111
[85] J.D. Pritts, M.S. Hursey, J.L. Michalek, S. Batelu, T.L. Stemmler, S.L.J. Michel, Unraveling the RNA Binding Properties of the Iron–Sulfur Zinc Finger Protein CPSF30, Biochemistry, 59, 8, (2020), 970-982, https://doi.org/10.1021/acs.biochem.9b01065
[86] J.D. Pritts, A.A. Oluyadi, W. Huang, G.D. Shimberg, M.A. Kane, A. Wilks, S.L.J. Michel, Understanding RNA Binding by the Nonclassical Zinc Finger Protein CPSF30, a Key Factor in Polyadenylation during Pre-mRNA Processing, Biochemistry, 60, 10, (2021), 780-790, https://doi.org/10.1021/acs.biochem.0c00940
[87] L. Schönemann, U. Kühn, G. Martin, P. Schäfer, A.R. Gruber, W. Keller, M. Zavolan, E. Wahle, Reconstitution of CPSF active in polyadenylation: recognition of the polyadenylation signal by WDR33, Genes Dev., 28, 21, (2014), 2381-2393, https://doi.org/10.1101/gad.250985.114
[88] J.W. Chang, H.S. Yeh, J. Yong, Alternative Polyadenylation in Human Diseases, Endocrinol. Metab., 32, 4, (2017), 413-421, https://doi.org/10.3803/EnM.2017.32.4.413
[89] S. Danckwardt, M.W. Hentze, A.E. Kulozik, 3' end mRNA processing: molecular mechanisms and implications for health and disease, EMBO J., 27, 3, (2008), 482-498, https://doi.org/10.1038/sj.emboj.7601932
[90] D.R. Higgs, S.E. Goodbourn, J. Lamb, J.B. Clegg, D.J. Weatherall, N.J. Proudfoot, Alpha-thalassaemia caused by a polyadenylation signal mutation, Nature, 306, 5941, (1983), 398-400, https://doi.org/10.1038/306398a0
[91] S.H. Orkin, T.C. Cheng, S.E. Antonarakis, H.H. Kazazian, Jr., Thalassemia due to a mutation in the cleavage-polyadenylation signal of the human beta-globin gene, EMBO J., 4, 2, (1985), 453-456,
[92] C.L. Bennett, M.E. Brunkow, F. Ramsdell, K.C. O'Briant, Q. Zhu, R.L. Fuleihan, A.O. Shigeoka, H.D. Ochs, P.F. Chance, A rare polyadenylation signal mutation of the FOXP3 gene (AAUAAA-->AAUGAA) leads to the IPEX syndrome, Immunogenetics, 53, 6, (2001), 435-439, https://doi.org/10.1007/s002510100358
[93] M. Yasuda, J. Shabbeer, M. Osawa, R.J. Desnick, Fabry disease: novel alpha-galactosidase A 3'-terminal mutations result in multiple transcripts due to aberrant

3'-end formation, Am. J. Hum. Genet., 73, 1, (2003), 162-173, https://doi.org/10.1086/376608
[94] R.E. Turner, A.D. Pattison, T.H. Beilharz, Alternative polyadenylation in the regulation and dysregulation of gene expression, Semin. Cell Dev. Biol., 75, 1096-3634 (Electronic), (2017), 61-69,
[95] A. Hellquist, M. Zucchelli, K. Kivinen, U. Saarialho-Kere, S. Koskenmies, E. Widen, H. Julkunen, A. Wong, M.L. Karjalainen-Lindsberg, T. Skoog, J. Vendelin, D.S. Cunninghame-Graham, T.J. Vyse, J. Kere, C.M. Lindgren, The human GIMAP5 gene has a common polyadenylation polymorphism increasing risk to systemic lupus erythematosus, J. Med. Genet., 44, 5, (2007), 314-321, https://doi.org/10.1136/jmg.2006.046185
[96] R.C. diTargiani, S.J. Lee, S. Wassink, S.L. Michel, Functional characterization of iron-substituted tristetraprolin-2D (TTP-2D, NUP475-2D): RNA binding affinity and selectivity, Biochemistry, 45, 45, (2006), 13641-13649, https://doi.org/10.1021/bi060747n
[97] S.L. Michel, A.L. Guerrerio, J.M. Berg, Selective RNA binding by a single CCCH zinc-binding domain from Nup475 (Tristetraprolin), Biochemistry, 42, 16, (2003), 4626-4630, https://doi.org/10.1021/bi034073h
[98] M. Lebendiker, T. Danieli, Purification of Proteins Fused to Maltose-Binding Protein, Methods Mol. Biol., 1485, (2017), 257-273, https://doi.org/10.1007/978-1-4939-6412-3_13
[99] M. Lebendiker, T. Danieli, Purification of proteins fused to maltose-binding protein, Methods Mol. Biol., 681, (2011), 281-293, https://doi.org/10.1007/978-1-60761-913-0_15
[100] S. De Franco, J. Vandenameele, A. Brans, O. Verlaine, K. Bendak, C. Damblon, A. Matagne, D.J. Segal, M. Galleni, J.P. Mackay, M. Vandevenne, Exploring the suitability of RanBP2-type Zinc Fingers for RNA-binding protein design, Sci. Rep., 9, 1, (2019), 2484, https://doi.org/10.1038/s41598-019-38655-y
[101] C.D. Trainor, R. Ghirlando, M.A. Simpson, GATA zinc finger interactions modulate DNA binding and transactivation, J. Biol. Chem., 275, 36, (2000), 28157-28166, https://doi.org/10.1074/jbc.M000020200
[102] G.D. Shimberg, J.D. Pritts, S.L.J. Michel, Iron-Sulfur Clusters in Zinc Finger Proteins, Methods Enzymol., 599, (2018), 101-137, https://doi.org/10.1016/bs.mie.2017.09.005
[103] M.H. Sazinsky, B. LeMoine, M. Orofino, R. Davydov, K.Z. Bencze, T.L. Stemmler, B.M. Hoffman, J.M. Arguello, A.C. Rosenzweig, Characterization and structure of a Zn2+ and [2Fe-2S]-containing copper chaperone from Archaeoglobus fulgidus, J. Biol. Chem., 282, 35, (2007), 25950-25959, https://doi.org/10.1074/jbc.M703311200
[104] R.G. Dastidar, J. Hooda, A. Shah, T.M. Cao, R.M. Henke, L. Zhang, The nuclear localization of SWI/SNF proteins is subjected to oxygen regulation, Cell Biosci., 2, (2012), 30-30, https://doi.org/10.1186/2045-3701-2-30
[105] Z. Li, R. Wang, Y. Gao, C. Wang, L. Zhao, N. Xu, K.-E. Chen, S. Qi, M. Zhang, Y.-F. Tsay, N.M. Crawford, Y. Wang, The Arabidopsis CPSF30-L gene plays an essential role in nitrate signaling and regulates the nitrate transceptor gene NRT1.1, New Phytol., 216, 4, (2017), 1205-1222, https://doi.org/https://doi.org/10.1111/nph.14743
[106] J. Zhang, B. Addepalli, K.-Y. Yun, A.G. Hunt, R. Xu, S. Rao, Q.Q. Li, D.L. Falcone, A polyadenylation factor subunit implicated in regulating oxidative signaling in Arabidopsis thaliana, PloS one, 3, 6, (2008), e2410-e2410, https://doi.org/10.1371/journal.pone.0002410

[107] B. Addepalli, A.G. Hunt, Redox and heavy metal effects on the biochemical activities of an Arabidopsis polyadenylation factor subunit, Arch. Biochem. Biophys., 473, 1, (2008), 88-95, https://doi.org/https://doi.org/10.1016/j.abb.2008.02.027
[108] Y. Gao, L. Yan, Y. Huang, F. Liu, Y. Zhao, L. Cao, T. Wang, Q. Sun, Z. Ming, L. Zhang, J. Ge, L. Zheng, Y. Zhang, H. Wang, Y. Zhu, C. Zhu, T. Hu, T. Hua, B. Zhang, X. Yang, J. Li, H. Yang, Z. Liu, W. Xu, L.W. Guddat, Q. Wang, Z. Lou, Z. Rao, Structure of the RNA-dependent RNA polymerase from COVID-19 virus, Science, 368, 6492, (2020), 779-782, https://doi.org/doi:10.1126/science.abb7498
[109] H.S. Hillen, G. Kokic, L. Farnung, C. Dienemann, D. Tegunov, P. Cramer, Structure of replicating SARS-CoV-2 polymerase, Nature, 584, 7819, (2020), 154-156, https://doi.org/10.1038/s41586-020-2368-8
[110] J. Chen, B. Malone, E. Llewellyn, M. Grasso, P.M.M. Shelton, P.D.B. Olinares, K. Maruthi, E.T. Eng, H. Vatandaslar, B.T. Chait, T.M. Kapoor, S.A. Darst, E.A. Campbell, Structural Basis for Helicase-Polymerase Coupling in the SARS-CoV-2 Replication-Transcription Complex, Cell, 182, 6, (2020), 1560-1573.e1513, https://doi.org/10.1016/j.cell.2020.07.033
[111] W. Yin, C. Mao, X. Luan, D.D. Shen, Q. Shen, H. Su, X. Wang, F. Zhou, W. Zhao, M. Gao, S. Chang, Y.C. Xie, G. Tian, H.W. Jiang, S.C. Tao, J. Shen, Y. Jiang, H. Jiang, Y. Xu, S. Zhang, Y. Zhang, H.E. Xu, Structural basis for inhibition of the RNA-dependent RNA polymerase from SARS-CoV-2 by remdesivir, Science, 368, 6498, (2020), 1499-1504, https://doi.org/10.1126/science.abc1560
[112] M.C. Ghosh, W.H. Tong, D. Zhang, H. Ollivierre-Wilson, A. Singh, M.C. Krishna, J.B. Mitchell, T.A. Rouault, Tempol-mediated activation of latent iron regulatory protein activity prevents symptoms of neurodegenerative disease in IRP2 knockout mice, Proc. Natl. Acad. Sci. U. S. A., 105, 33, (2008), 12028-12033, https://doi.org/10.1073/pnas.0805361105
[113] M.C. Ghosh, D.L. Zhang, H. Ollivierre, M.A. Eckhaus, T.A. Rouault, Translational repression of HIF2alpha expression in mice with Chuvash polycythemia reverses polycythemia, J. Clin. Invest., 128, 4, (2018), 1317-1325, https://doi.org/10.1172/JCI97684
[114] L.Y. Chao, M.A. Marletta, J. Rine, Sre1, an iron-modulated GATA DNA-binding protein of iron-uptake genes in the fungal pathogen Histoplasma capsulatum, Biochemistry, 47, 27, (2008), 7274-7283, https://doi.org/10.1021/bi800066s
[115] J.-M. Moulis, Cellular Dynamics of Transition Metal Exchange on Proteins: A Challenge but a Bonanza for Coordination Chemistry, Biomolecules, 10, 11, (2020), 1584, https://doi.org/https://doi.org/10.3390/biom10111584
[116] J.R. Wiśniewski, M.Y. Hein, J. Cox, M. Mann, A “Proteomic Ruler” for Protein Copy Number and Concentration Estimation without Spike-in Standards*, Mol. Cell. Proteomics, 13, 12, (2014), 3497-3506, https://doi.org/https://doi.org/10.1074/mcp.M113.037309
[117] C.-A. Lo, I. Kays, F. Emran, T.-J. Lin, V. Cvetkovska, Brian E. Chen, Quantification of Protein Levels in Single Living Cells, Cell Rep., 13, 11, (2015), 2634-2644, https://doi.org/https://doi.org/10.1016/j.celrep.2015.11.048
[118] P.C. Dos Santos, D.C. Johnson, B.E. Ragle, M.C. Unciuleac, D.R. Dean, Controlled expression of nif and isc iron-sulfur protein maturation components reveals target specificity and limited functional replacement between the two systems, J. Bacteriol., 189, 7, (2007), 2854-2862, https://doi.org/10.1128/jb.01734-06
[119] R.M. McCarty, C. Krebs, V. Bandarian, Spectroscopic, steady-state kinetic, and mechanistic characterization of the radical SAM enzyme QueE, which catalyzes a

complex cyclization reaction in the biosynthesis of 7-deazapurines, Biochemistry, 52, 1, (2013), 188-198, https://doi.org/10.1021/bi301156w
[120] J.L. Thweatt, B.H. Ferlez, J.H. Golbeck, D.A. Bryant, BciD Is a Radical S-Adenosyl-l-methionine (SAM) Enzyme That Completes Bacteriochlorophyllide e Biosynthesis by Oxidizing a Methyl Group into a Formyl Group at C-7, J. Biol. Chem., 292, 4, (2017), 1361-1373, https://doi.org/10.1074/jbc.M116.767665
[121] S. Barber-Zucker, B. Shaanan, R. Zarivach, Transition metal binding selectivity in proteins and its correlation with the phylogenomic classification of the cation diffusion facilitator protein family, Sci. Rep., 7, 1, (2017), 16381, https://doi.org/10.1038/s41598-017-16777-5
[122] A.N. Albetel, C.E. Outten, Characterization of Glutaredoxin Fe-S Cluster-Binding Interactions Using Circular Dichroism Spectroscopy, Methods Enzymol., 599, (2018), 327-353, https://doi.org/10.1016/bs.mie.2017.11.003
[123] G.L. Miessler, D.A. Tarr, Inorganic Chemistry, 2nd Edition, (2004),
[124] D.F. Shriver, P.W. Atkins, C.H. Langford, Inorganic chemistry (1994)
[125] S.E. Evans, S.L. Michel, Dissecting the role of DNA sequence in Helicobacter pylori NikR/DNA recognition, Dalton Trans., 41, 26, (2012), 7946-7951, https://doi.org/10.1039/c2dt30504f
[126] H.M. Neu, S.A. Alexishin, J.E.P. Brandis, A.M.C. Williams, W. Li, D. Sun, N. Zheng, W. Jiang, A. Zimrin, J.C. Fink, J.E. Polli, M.A. Kane, S.L.J. Michel, Snapshots of Iron Speciation: Tracking the Fate of Iron Nanoparticle Drugs via a Liquid Chromatography-Inductively Coupled Plasma-Mass Spectrometric Approach, Mol. Pharm., 16, 3, (2019), 1272-1281, https://doi.org/10.1021/acs.molpharmaceut.8b01215
[127] G.D. Shimberg, K. Ok, H.M. Neu, K.E. Splan, S.L.J. Michel, Cu(I) Disrupts the Structure and Function of the Nonclassical Zinc Finger Protein Tristetraprolin (TTP), Inorg. Chem., 56, 12, (2017), 6838-6848, https://doi.org/10.1021/acs.inorgchem.7b00125
[128] K. Ok, W. Li, H.M. Neu, S. Batelu, T.L. Stemmler, M.A. Kane, S.L.J. Michel, Role of Gold in Inflammation and Tristetraprolin Activity, Chemistry, 26, 7, (2020), 1535-1547, https://doi.org/10.1002/chem.201904837
[129] J.L. Michalek, S.J. Lee, S.L. Michel, Cadmium coordination to the zinc binding domains of the non-classical zinc finger protein Tristetraprolin affects RNA binding selectivity, J. Inorg. Biochem., 112, (2012), 32-38, https://doi.org/10.1016/j.jinorgbio.2012.02.023
[130] J.E.P. Brandis, S.M. Zalesak, M.A. Kane, S.L.J. Michel, Cadmium Exchange with Zinc in the Non-Classical Zinc Finger Protein Tristetraprolin, Inorg. Chem., 60, 11, (2021), 7697-7707, https://doi.org/10.1021/acs.inorgchem.0c03808
[131] M.L. Zastrow, V.L. Pecoraro, Designing hydrolytic zinc metalloenzymes, Biochemistry, 53, 6, (2014), 957-978, https://doi.org/10.1021/bi4016617
[132] R.T. Doku, G. Park, K.E. Wheeler, K.E. Splan, Spectroscopic characterization of copper(I) binding to apo and metal-reconstituted zinc finger peptides, J. Biol. Inorg. Chem., 18, 6, (2013), 669-678, https://doi.org/10.1007/s00775-013-1012-6
[133] J.S. Magyar, T.C. Weng, C.M. Stern, D.F. Dye, B.W. Rous, J.C. Payne, B.M. Bridgewater, A. Mijovilovich, G. Parkin, J.M. Zaleski, J.E. Penner-Hahn, H.A. Godwin, Reexamination of lead(II) coordination preferences in sulfur-rich sites: implications for a critical mechanism of lead poisoning, J. Am. Chem. Soc., 127, 26, (2005), 9495-9505, https://doi.org/10.1021/ja0424530
[134] J. Li, X. Ren, B. Fan, Z. Huang, W. Wang, H. Zhou, Z. Lou, H. Ding, J. Lyu, G. Tan, Zinc toxicity and iron-sulfur cluster biogenesis in Escherichia coli, Appl. Environ. Microbiol., (2019), https://doi.org/10.1128/AEM.01967-18

[135] M. Huang, D. Krepkiy, W. Hu, D.H. Petering, Zn-, Cd-, and Pb-transcription factor IIIA: properties, DNA binding, and comparison with TFIIIA-finger 3 metal complexes, J. Inorg. Biochem., 98, 5, (2004), 775-785, https://doi.org/10.1016/j.jinorgbio.2004.01.014
[136] S.C. Gill, P.H. von Hippel, Calculation of protein extinction coefficients from amino acid sequence data, Anal. Biochem., 182, 2, (1989), 319-326, https://doi.org/https://doi.org/10.1016/0003-2697(89)90602-7
[137] M.N. Berberan-Santos, Beer's law revisited, J. Chem. Educ., 67, 9, (1990), 757, https://doi.org/10.1021/ed067p757
[138] B. Holmquist, B.L. Vallee, Metal-coordinating substrate analogs as inhibitors of metalloenzymes, Proc. Natl. Acad. Sci. U. S. A., 76, 12, (1979), 6216-6220, https://doi.org/10.1073/pnas.76.12.6216
[139] H. Beinert, R.H. Sands, Studies on succinic and DPNH dehydrogenase preparations by paramagnetic resonance (EPR) spectroscopy, Biochem. Biophys. Res. Commun., 3, 1, (1960), 41-46, https://doi.org/https://doi.org/10.1016/0006-291X(60)90100-5
[140] T.A. Rouault, Iron-sulfur proteins hiding in plain sight, Nat. Chem. Biol., 11, 7, (2015), 442-445, https://doi.org/10.1038/nchembio.1843
[141] J.G. Norman Jr, P.B. Ryan, L. Noodleman, Electronic structure of 2-Fe ferredoxin models by X. alpha. valence bond theory, J. Am. Chem. Soc., 102, 12, (1980), 4279-4282, https://doi.org/https://doi.org/10.1021/ja00532a060
[142] L. Noodleman, E.J. Baerends, Electronic structure, magnetic properties, ESR, and optical spectra for 2-iron ferredoxin models by LCAO-X. alpha. valence bond theory, J. Am. Chem. Soc., 106, 8, (1984), 2316-2327, https://doi.org/https://doi.org/10.1021/ja00320a017
[143] A. Aizman, D.A. Case, Electronic structure calculations on active site models for 4-Fe, 4-S iron-sulfur proteins, J. Am. Chem. Soc., 104, 12, (1982), 3269-3279,
[144] A. Kubas, Characterization of charge transfer excited states in [2Fe–2S] iron–sulfur clusters using conventional configuration interaction techniques, Theor. Chem. Acc., 139, 7, (2020), 120, https://doi.org/10.1007/s00214-020-02635-7
[145] K.S. Hagen, A.D. Watson, R.H. Holm, Synthetic routes to iron sulfide (Fe2S2, Fe3S4, Fe4S4, and Fe6S9), clusters from the common precursor tetrakis(ethanethiolate)ferrate(2-) ion ([Fe(SC2H5)4]2-): structures and properties of [Fe3S4(SR)4]3- and bis(ethanethiolate)nonathioxohexaferrate(4-) ion ([Fe6S9(SC2H5)2]4-), examples of the newest types of Fe-S-SR clusters, J. Am. Chem. Soc., 105, 12, (1983), 3905-3913, https://doi.org/10.1021/ja00350a028
[146] S.A. Latt, B.L. Vallee, Spectral properties of cobalt carboxypeptidase. Effects of substrates and inhibitors, Biochemistry, 10, 23, (1971), 4263-4270, https://doi.org/10.1021/bi00799a017
[147] J.M. Berg, D.L. Merkle, On the metal ion specificity of zinc finger proteins, J. Am. Chem. Soc., 111, 10, (1989), 3759-3761, https://doi.org/10.1021/ja00192a050
[148] A.Z. Mason, S.D. Storms, K.D. Jenkins, Metalloprotein separation and analysis by directly coupled size exclusion high-performance liquid chromatography inductively coupled plasma mass spectroscopy, Anal. Biochem., 186, 2, (1990), 187-201, https://doi.org/10.1016/0003-2697(90)90066-i
[149] A. Lothian, B.R. Roberts, Standards for Quantitative Metalloproteomic Analysis Using Size Exclusion ICP-MS, J. Vis. Exp., 110, (2016), https://doi.org/10.3791/53737
[150] X. Xu, H. Wang, H. Li, H. Sun, Metalloproteomic Approaches for Matching Metals to Proteins: The Power of Inductively Coupled Plasma Mass Spectrometry (ICP-MS), Chem. Lett., 49, 6, (2020), 697-704, https://doi.org/10.1246/cl.200155

[151] R. Lobinski, D. Schaumloffel, J. Szpunar, Mass spectrometry in bioinorganic analytical chemistry, Mass. Spectrom. Rev., 25, 2, (2006), 255-289, https://doi.org/10.1002/mas.20069
[152] J.E. Penner-Hahn, X-ray absorption spectroscopy in coordination chemistry, Coord. Chem. Rev., 190-192, (1999), 1101-1123, https://doi.org/https://doi.org/10.1016/S0010-8545(99)00160-5
[153] R.A. Scott, C.M. Lukehart, Applications of physical methods to inorganic and bioinorganic chemistry (2007)
[154] W. Shi, M. Punta, J. Bohon, J.M. Sauder, R. D'Mello, M. Sullivan, J. Toomey, D. Abel, M. Lippi, A. Passerini, P. Frasconi, S.K. Burley, B. Rost, M.R. Chance, Characterization of metalloproteins by high-throughput X-ray absorption spectroscopy, Genome Res., 21, 6, (2011), 898-907, https://doi.org/10.1101/gr.115097.110
[155] L. Zhang, in: Y. Hu (Ed.), Metalloproteins: Methods and Protocols, Springer New York, New York, NY, (2019), pp. 179-195.
[156] C.D. Garner, XAS studies of metal centres in proteins, Phys. B, 208-209, (1995), 714-716, https://doi.org/https://doi.org/10.1016/0921-4526(94)00892-Y
[157] G.N. George, B. Hedman, K.O. Hodgson, An edge with XAS, Nat. Struct. Biol., 5, 8, (1998), 645-647, https://doi.org/10.1038/1336
[158] H. Li, D.T. Mapolelo, N.N. Dingra, S.G. Naik, N.S. Lees, B.M. Hoffman, P.J. Riggs-Gelasco, B.H. Huynh, M.K. Johnson, C.E. Outten, The Yeast Iron Regulatory Proteins Grx3/4 and Fra2 Form Heterodimeric Complexes Containing a [2Fe-2S] Cluster with Cysteinyl and Histidyl Ligation, Biochemistry, 48, 40, (2009), 9569-9581, https://doi.org/10.1021/bi901182w
[159] A. Kounosu, Z. Li, N.J. Cosper, J.E. Shokes, R.A. Scott, T. Imai, A. Urushiyama, T. Iwasaki, Engineering a three-cysteine, one-histidine ligand environment into a new hyperthermophilic archaeal Rieske-type [2Fe-2S] ferredoxin from Sulfolobus solfataricus, J. Biol. Chem., 279, 13, (2004), 12519-12528, https://doi.org/10.1074/jbc.M305923200
[160] A. Jasniewski, Y. Hu, M.W. Ribbe, Electron Paramagnetic Resonance Spectroscopy of Metalloproteins, Methods Mol. Biol., 1876, (2019), 197-211, https://doi.org/10.1007/978-1-4939-8864-8_13
[161] C. More, V. Belle, M. Asso, A. Fournel, G. Roger, B. Guigliarelli, P. Bertrand, EPR spectroscopy: A powerful technique for the structural and functional investigation of metalloproteins, Biospectroscopy, 5, S5, (1999), S3-S18, https://doi.org/https://doi.org/10.1002/(SICI)1520-6343(1999)5:5
[162] D.J. Lowe, ENDOR and EPR of metalloproteins, Prog. Biophys. Mol. Biol., 57, 1, (1992), 1-22, https://doi.org/https://doi.org/10.1016/0079-6107(92)90002-N
[163] W.R. Hagen, EPR spectroscopy of complex biological iron-sulfur systems, J. Biol. Inorg. Chem., 23, 4, (2018), 623-634, https://doi.org/10.1007/s00775-018-1543-y
[164] W.R. Hagen, EPR spectroscopy as a probe of metal centres in biological systems, Dalton Trans., 37, (2006), 4415-4434, https://doi.org/10.1039/B608163K
[165] W.R. Hagen, in: R. Cammack (Ed.), Adv. Inorg. Chem., vol. 38, Academic Press, (1992), pp. 165-222.
[166] G.E. Cutsail, 3rd, J. Telser, B.M. Hoffman, Advanced paramagnetic resonance spectroscopies of iron-sulfur proteins: Electron nuclear double resonance (ENDOR) and electron spin echo envelope modulation (ESEEM), Biochim. Biophys. Acta, 1853, 6, (2015), 1370-1394, https://doi.org/10.1016/j.bbamcr.2015.01.025

[167] M.-E. Pandelia, N.D. Lanz, S.J. Booker, C. Krebs, Mössbauer spectroscopy of Fe/S proteins, Biochim. Biophys. Acta - Mol. Cell Res., 1853, 6, (2015), 1395-1405, https://doi.org/https://doi.org/10.1016/j.bbamcr.2014.12.005
[168] D.T. Mapolelo, B. Zhang, S.G. Naik, B.H. Huynh, M.K. Johnson, Spectroscopic and functional characterization of iron-sulfur cluster-bound forms of Azotobacter vinelandii (Nif)IscA, Biochemistry, 51, 41, (2012), 8071-8084, https://doi.org/10.1021/bi3006658
[169] W.R. Dunham, L.J. Harding, R.H. Sands, Mössbauer spectroscopy of metalloproteins and the use of Fourier transforms, Eur. J. Biochem., 214, 1, (1993), 1-8, https://doi.org/10.1111/j.1432-1033.1993.tb17889.x
[170] Y. Gao, C. Chen, Z. Chai, Advanced nuclear analytical techniques for metalloproteomics, J. Anal. At. Spectrom., 22, 8, (2007), 856-866, https://doi.org/10.1039/B703323K
[171] A.A. Kamnev, A.V. Tugarova, Sample treatment in Mössbauer spectroscopy for protein-related analyses: Nondestructive possibilities to look inside metal-containing biosystems, Talanta, 174, (2017), 819-837, https://doi.org/https://doi.org/10.1016/j.talanta.2017.06.057
[172] T.F. Tirrell, M.L. Paddock, A.R. Conlan, E.J. Smoll, R. Nechushtai, P.A. Jennings, J.E. Kim, Resonance Raman Studies of the (His)(Cys)3 2Fe-2S Cluster of MitoNEET: Comparison to the (Cys)4 Mutant and Implications of the Effects of pH on the Labile Metal Center, Biochemistry, 48, 22, (2009), 4747-4752, https://doi.org/10.1021/bi900028r
[173] R.S. Czernusxewicx, in: C. Jones, B. Mulloy, A.H. Thomas (Eds.), Spectroscopic Methods and Analyses: NMR, Mass Spectrometry, and Metalloprotein Techniques, Humana Press, Totowa, NJ, (1993), pp. 345-374.
[174] T.G. Spiro, R.S. Czernuszewicz, Resonance Raman spectroscopy of metalloproteins, Methods Enzymol., 246, (1995), 416-460,
[175] S. Todorovic, M. Teixeira, Resonance Raman spectroscopy of Fe–S proteins and their redox properties, JBIC, J. Biol. Inorg. Chem., 23, 4, (2018), 647-661, https://doi.org/10.1007/s00775-018-1533-0
[176] P.J. Stephens, A.J. Thomson, J.B.R. Dunn, T.A. Keiderling, J. Rawlings, K.K. Rao, D.O. Hall, Circular dichroism and magnetic circular dichroism of iron-sulfur proteins, Biochemistry, 17, 22, (1978), 4770-4778, https://doi.org/10.1021/bi00615a026
[177] M.T. Pellicer Martinez, J.C. Crack, M.Y. Stewart, J.M. Bradley, D.A. Svistunenko, A.W. Johnston, M.R. Cheesman, J.D. Todd, N.E. Le Brun, Mechanisms of iron- and O2-sensing by the [4Fe-4S] cluster of the global iron regulator RirA, eLife, 8, (2019), https://doi.org/10.7554/eLife.47804
[178] J.C. Crack, E. Gray, N.E. Le Brun, Sensing mechanisms of iron-sulfur cluster regulatory proteins elucidated using native mass spectrometry, Dalton Trans., 50, 23, (2021), 7887-7897, https://doi.org/10.1039/d1dt00993a
[179] S. Garza, P.W. Thomas, W. Fast, M. Moini, Metal displacement and stoichiometry of protein-metal complexes under native conditions using capillary electrophoresis/mass spectrometry, Rapid Commun. Mass Spectrom., 24, 18, (2010), 2730-2734, https://doi.org/10.1002/rcm.4702
[180] E.M. Martin, F.D.L. Kondrat, A.J. Stewart, J.H. Scrivens, P.J. Sadler, C.A. Blindauer, Native electrospray mass spectrometry approaches to probe the interaction between zinc and an anti-angiogenic peptide from histidine-rich glycoprotein, Sci. Rep., 8, 1, (2018), 8646, https://doi.org/10.1038/s41598-018-26924-1

[181] J.C. Crack, N.E. Le Brun, Native Mass Spectrometry of Iron-Sulfur Proteins, Methods Mol. Biol., 2353, (2021), 231-258, https://doi.org/10.1007/978-1-0716-1605-5_13
[182] Y. Lu, N. Yeung, N. Sieracki, N.M. Marshall, Design of functional metalloproteins, Nature, 460, 7257, (2009), 855-862, https://doi.org/10.1038/nature08304
[183] J.M. Moulis, V. Davasse, M.-P. Golinelli, J. Meyer, I. Quinkal, The coordination sphere of iron-sulfur clusters: lessons from site-directed mutagenesis experiments, JBIC, J. Biol. Inorg. Chem., 1, 1, (1996), 2-14, https://doi.org/10.1007/s007750050017
[184] R.H. Holm, W. Lo, Structural Conversions of Synthetic and Protein-Bound Iron-Sulfur Clusters, Chem. Rev., 116, 22, (2016), 13685-13713, https://doi.org/10.1021/acs.chemrev.6b00276
[185] P. Venkateswara Rao, R.H. Holm, Synthetic analogues of the active sites of iron-sulfur proteins, Chem. Rev., 104, 2, (2004), 527-559, https://doi.org/10.1021/cr020615+
[186] H. Beinert, R.H. Holm, E. Munck, Iron-sulfur clusters: nature's modular, multipurpose structures, Science, 277, 5326, (1997), 653-659, https://doi.org/DOI: 10.1126/science.277.5326.653
[187] A.W. Foster, D. Osman, N.J. Robinson, Metal preferences and metallation, J. Biol. Chem., 289, 41, (2014), 28095-28103, https://doi.org/10.1074/jbc.R114.588145
[188] A.W. Foster, T.R. Young, P.T. Chivers, N.J. Robinson, Protein metalation in biology, Curr. Opin. Chem. Biol., 66, (2022), 102095, https://doi.org/https://doi.org/10.1016/j.cbpa.2021.102095
[189] K.A. Edmonds, M.R. Jordan, D.P. Giedroc, COG0523 proteins: a functionally diverse family of transition metal-regulated G3E P-loop GTP hydrolases from bacteria to man, Metallomics, 13, 8, (2021), https://doi.org/10.1093/mtomcs/mfab046
[190] T.A. Rouault, Mammalian iron–sulphur proteins: novel insights into biogenesis and function, Nat. Rev. Mol. Cell Biol., 16, 1, (2015), 45-55, https://doi.org/10.1038/nrm3909
[191] B. Py, F. Barras, Genetic approaches of the Fe–S cluster biogenesis process in bacteria: Historical account, methodological aspects and future challenges, Biochim. Biophys. Acta, Mol. Cell Res., 1853, 6, (2015), 1429-1435, https://doi.org/https://doi.org/10.1016/j.bbamcr.2014.12.024
[192] M.R. Jordan, J. Wang, A. Weiss, E.P. Skaar, D.A. Capdevila, D.P. Giedroc, Mechanistic Insights into the Metal-Dependent Activation of Zn(II)-Dependent Metallochaperones, Inorg. Chem., 58, 20, (2019), 13661-13672, https://doi.org/10.1021/acs.inorgchem.9b01173
[193] A. Krężel, W. Maret, The Bioinorganic Chemistry of Mammalian Metallothioneins, Chem. Rev., 121, 23, (2021), 14594-14648, https://doi.org/10.1021/acs.chemrev.1c00371
[194] V. Van, J.B. Brown, H. Rosenbach, I. Mohamed, N.-E. Ejimogu, T.S. Bui, V.A. Szalai, K.N. Chacón, I. Span, A.T. Smith, Iron-sulfur clusters are involved in post-translational arginylation, bioRxiv, (2021), 2021.2004.2013.439645, https://doi.org/10.1101/2021.04.13.439645